IEEE Access
Multidisciplinary ⋮ Rapid Review ⋮ Open Access Journal

Received 14 January 2023, accepted 4 February 2023, date of publication 9 February 2023, date of current version 14 February 2023.

Digital Object Identifier 10.1109/ACCESS.2023.3243635

RESEARCH ARTICLE

Strategies to Measure Soil Moisture Using Traditional Methods, Automated Sensors, Remote Sensing, and Machine Learning Techniques: Review, Bibliometric Analysis, Applications, Research Findings, and Future Directions

ABHILASH SINGH[1], (Member, IEEE), KUMAR GAURAV[1], GAURAV KAILASH SONKAR[1], AND CHENG-CHI LEE[2,3], (Member, IEEE)

[1]Fluvial Geomorphology and Remote Sensing Laboratory, Department of Earth and Environmental Sciences, Indian Institute of Science Education and Research Bhopal, Madhya Pradesh, Bhopal 462066, India
[2]Research and Development Center for Physical Education, Health, and Information Technology, Department of Library and Information Science, Fu Jen Catholic University, New Taipei City 24205, Taiwan
[3]Department of Computer Science and Information Engineering, Asia University, Wufeng, Taichung 41354, Taiwan

Corresponding authors: Kumar Gaurav (kgaurav@iiserb.ac.in) and Cheng-Chi Lee (cclee@mail.fju.edu.tw)

Kumar Gaurav acknowledges the Space Application Center-Indian Space Research Organisation (SAC-ISRO) for the funding support through Grant Hyd-01. Abhilash Singh acknowledges the Department of Science and Technology (DST), Government of India, for providing a DST-Innovation in Science Pursuit for Inspired Research (INSPIRE) fellowship through Grant No. DST/INSPIRE Fellowship/[IF180001] to pursue Ph.D. at IISER Bhopal.

ABSTRACT This review provides a detailed synthesis of various in-situ, remote sensing, and machine learning approaches to estimate soil moisture. Bibliometric analysis of the published literature on soil moisture shows that Time-Domain Reflectometry (TDR) is the most widely used in-situ instrument, while remote sensing is the most preferred application, and random forest is the widely applied algorithm to simulate surface soil moisture. We have applied ten most widely used machine learning models on a publicly available dataset (in-situ soil moisture measurement and satellite images) to predict soil moisture and compared their results. We have briefly discussed the potential of using the upcoming NASA-ISRO Synthetic Aperture Radar (NISAR) mission images to estimate soil moisture. Finally, this review discusses the capabilities of physics-informed and automated machine learning (AutoML) models to predict the surface soil moisture at higher spatial and temporal resolutions. This review will assist researchers in investigating the applications of soil moisture in the broad domain of earth sciences.

INDEX TERMS Surface soil moisture, bibliometric analysis, machine learning, remote sensing, NISAR, AutoML.

I. INTRODUCTION

Soil moisture is a temporary storage of water in the soil pores [1], [2]. This fraction of water seems negligible (0.0012%) as compared to the water available on the earth, but it is crucial for the hydrological cycle and the biological processes at the air-soil interface [3], [4], [5], [6], [7]. The study of spatial and temporal variation of soil moisture is crucial for different applications such as the prediction of the flood, drought, and forest fire & climate and agriculture investigations [8], [9], [10], [11], [12], [13]. Soil moisture can be estimated/measured at different spatial (local and global) scales. At the local scale, it is generally measured in the field by using different direct and indirect methods depending on the measurement techniques. The amount of moisture content in a soil sample is traditionally measured by using the direct

The associate editor coordinating the review of this manuscript and approving it for publication was Kuan Chee.

method (*i.e.,* oven dry method). The soil sample is fully dried in an oven; the difference between the initial and dry weight of the soil sample gives the moisture content. This method is destructive, time-consuming, and provides soil moisture only at discrete locations. Later indirect methods based on automated sensors, such as theta probes, were developed to estimate soil moisture. Such indirect methods can measure the moisture of a soil column at different depths at discrete locations.

Satellite images (such as Sentinel-1, Sentinel-2, and Radarsat-2) provide synoptic coverage of the earth's surface at different spatial and temporal resolutions. Due to these capabilities, microwaves together with the optical remote sensing satellite images, have been proven useful for monitoring surface soil moisture at the global and regional scales [20], [21], [22], [23]. The European Space Agency (ESA), under the ESA-EO mission, launched Soil Moisture and Ocean Salinity (SMOS) mission in 2009. Later the Soil Moisture Active Passive (SMAP) was launched in 2015, by the National Aeronautics and Space Administration (NASA) under Earth System Science Pathfinder (ESSP) mission. These satellite missions provide moisture products on a daily to eight days revisit time, at the spatial resolution varying from 1 $\sim$ 50 km. The soil moisture product of these satellite missions has data void, particularly at the locations of complex topography and dense vegetation [24], [25].

Microwave remote sensing images have been widely used for estimating soil moisture due to their penetration capacity to the top soil layer and their sensitivity towards dielectric properties of the material [26], [27]. The microwave signals exhibit a permittivity (ϵ) gradient between dry soil ($\sim$ 2) and water ($\sim$ 80) [28], [29], [30]. Various backscattering models (*i.e.,* theoretical, empirical, and semi-empirical) have been developed to model soil moisture from microwave images [31], [32], [33], [34], [35], [36], [37], [38], [39], [40]. These models require quad-polarised (VV, VH, HH, and HV) microwave images. The quad-polarised microwave images are often not available for some regions. For example, the publicly accessible Sentinel-1 images, for most countries, are available only in dual polarisation [41]. To overcome this limitation, data-driven models (*i.e.,* machine learning) have been proposed to predict soil moisture by using the backscatter values in different polarisation and other ancillary data (topography, vegetation indices, etc.) as input features. This approach initially requires in-situ soil moisture to train and test the machine learning models. Once the model is trained, it can be used to predict soil moisture just by using a set of input variables discussed above.

Few review papers have been published so far discussing the in-situ soil moisture estimation methods. We have tabulated these studies in Table 1. McKim et al. [14] presented a brief review of gravimetric, nuclear, electromagnetic, tensiometric, and hygroscopic methods and their pros and cons, with special emphasis on tensiometric and electromagnetic methods. Similarly, Zazueta and Xin [16], presented a brief review of gravimetric, nuclear, and electromagnetic methods with their associated pros and cons. Stafford [15], carried out a systematic review on remote, non-contact, and in-situ methods of soil moisture estimation. Ling [17] presented a short review on tensiometers, granular matrix sensors, dielectric sensors, and heat-dissipating sensors for soil moisture measurements with the advantages and disadvantages of each sensor. Su et al. [18] reviewed the state-of-the-art soil moisture measurement techniques. In addition, they also reviewed the impact of various soil-specific parameters on soil moisture measurements. Recently, Hardie [19], reviewed the existing and emerging soil moisture sensors that are preferably used. To the best of our knowledge, none of the above-discussed reviews have performed bibliometric analysis that includes a review of the soil moisture sensors, remote sensing techniques, and machine learning algorithms. We could not find any review articles that synthesize the potential use of the in-situ measurements to develop remote sensing-based machine learning methods to estimate regional and global soil moisture (Table 1).

The use of machine learning models are increasing rapidly in almost every application due to their high computational efficiency. This reflects a sharp increase in publications on soil moisture estimation that includes machine learning models. About 537 publications (502 research - 502, review - 26, and data and editorial - 9) have been published from 1995 to 2022. From 2012 to 2022 (till 15th January 2022), we found 519 publications on the Web of Science (WoS) database (Figure 1). USA emerges as the highest contributor with 180 research publications, followed by China, Germany, India, and Canada. A majority of these publications have used in-situ measured soil moisture and satellite images to train and validate machine learning models. It would be useful to discuss the pros and cons of all the available methods and sensors which are generally used to collect the in-situ measurement along with the discussion of remote sensing-based machine learning approaches for soil moisture estimation.

This review first discusses the required theory together with the advantages and disadvantages of traditional and automated methods. Among the traditional methods, we discussed the gravimetric and volumetric methods in detail. Whereas in the automated methods, we have considered the radiological techniques (*i.e.,* neutron and gamma rays probe), soil-water dielectric techniques (*i.e.,* Time-Domain Reflectometry (TDR), and Frequency-Domain Reflectometry (FDR)), and soil-water potential techniques (*i.e.,* tensiometer, resistance block, and psychrometers). Following this, we have performed the bibliometric analysis of each method and sensor to analyse their relative usages. We then discussed various remote sensing techniques for soil moisture estimation, specifically by using microwave remote sensing. Lastly, we present a comprehensive comparison of the machine learning algorithms that are extensively used in soil moisture study.

TABLE 1. Summary of the existing review papers on soil moisture sensors. The ✓ and ✗ are to indicate the review scopes that have been covered and not covered, respectively.

Publication	One sentence summary	Scope				
		Sensors and methods			Bibliometric	Machine learning
		Theory	Pros	Cons	Analysis	Application
[14]	In-situ soil moisture methods	✓	✓	✓	✗	✗
[15]	Remote and in-situ soil moisture methods	✓	✓	✓	✗	✗
[16]	Soil moisture sensors	✓	✓	✓	✗	✗
[17]	Soil moisture sensors	✓	✓	✓	✗	✗
[18]	Soil moisture measurements	✓	✓	✓	✗	✗
[19]	Proximal soil moisture sensors	✓	✓	✓	✗	✗
This work	Soil moisture: In-situ and remote sensing for machine learning	✓	✓	✓	✓	✓

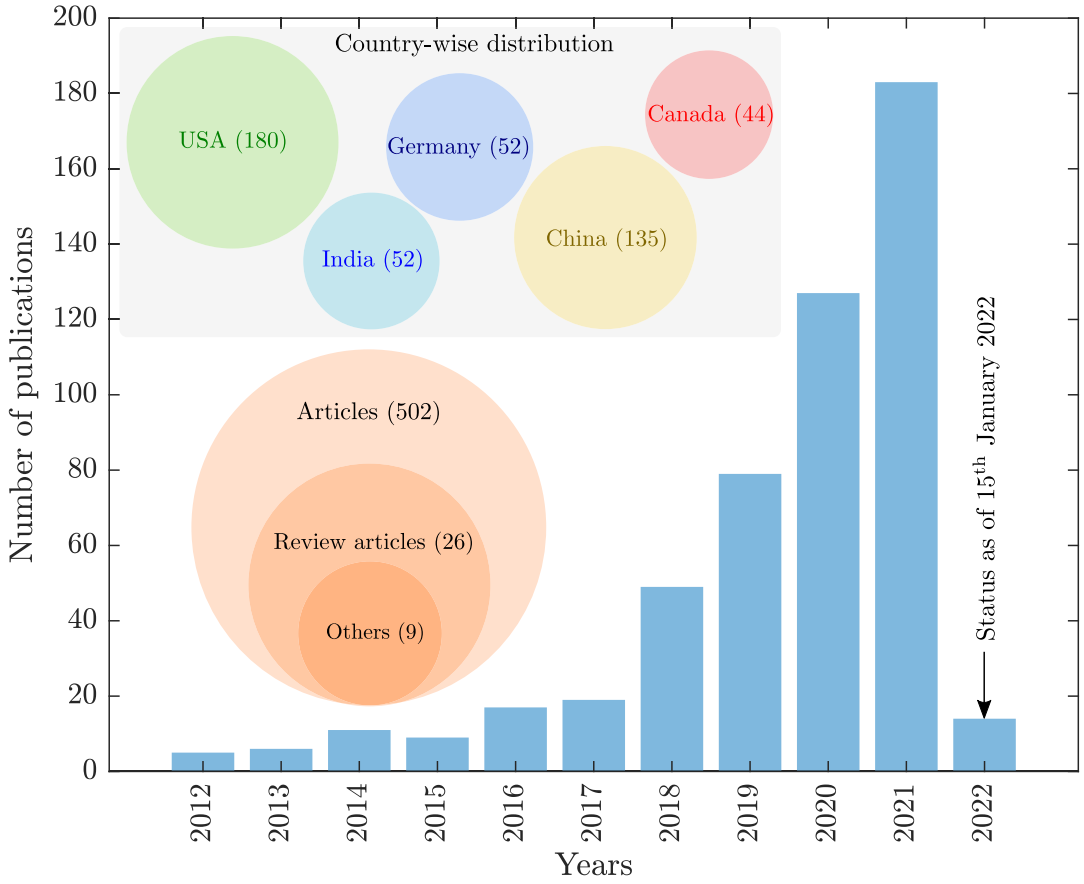

FIGURE 1. Number of publications (research articles, review papers, and others) from 2012 to 2022 on soil moisture together with the machine learning models from different countries.

This review work is organised into seven different sections. Section-I discusses the state-of-the-art techniques in soil moisture measurement, importance, and spatial scale. We have compared the existing reviews on soil moisture and finally highlighted the need for the present review. Section II provides a detailed review of in-situ instruments, remote sensing methods, and machine learning techniques to estimate soil moisture. We discussed different methods and sensors used for in-situ measurement of soil moisture (*i.e.,* oven-dry, radiological techniques, dielectric techniques, and potential techniques). We presented a review on the application of remote sensing images and machine learning models to estimate surface soil moisture. Finally, we provided a summary of each method and its key characteristics. Section III consists of a bibliometric analysis of the methods and sensors that are frequently used for collecting in-situ soil moisture measurements (*i.e.,* gravimetric, neutron probe, tensiometer, TDR, and FDR) and summarises the findings. Section IV is the bibliometric analysis of the application and algorithms (*i.e.,* remote sensing, random forest, neural network, and support vector machine) that are most frequently used in soil moisture studies. Section V

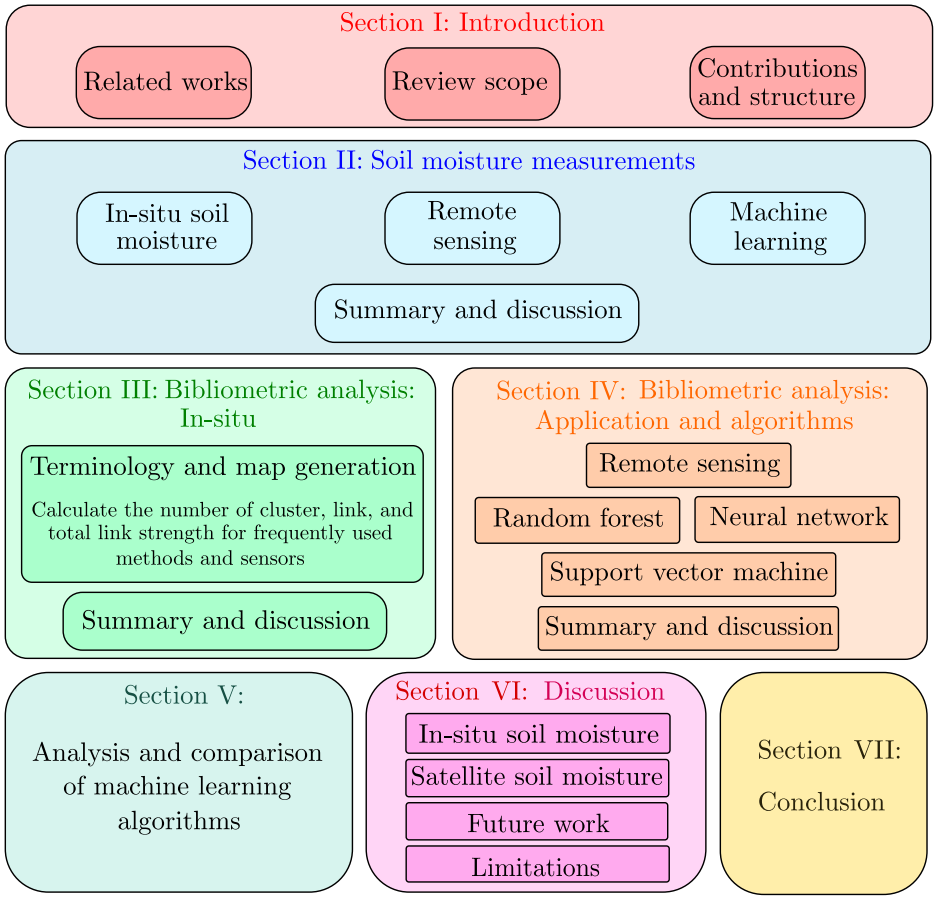

FIGURE 2. Road map of the review paper.

contains a comprehensive analysis of ten different machine learning algorithms that are widely used to model surface soil moisture. Sections VI and VII are about the overall analysis and summary of this review. Figure 2 illustrates the structure of the review work.

II. SOIL MOISTURE MEASUREMENTS

A. IN-SITU SOIL MOISTURE

In-situ measurements are classified into direct and indirect methods. Oven drying methods (both gravimetric and volumetric soil moisture) are the only direct methods for soil moisture determination; on the other hand, all the automated techniques for soil moisture estimation come under the indirect method. In the direct method, also known as a destructive method, soil moisture is estimated by drilling holes into the ground, disturbing the soil root zone and eventually affecting infiltration and drainage behaviour. In contrast, indirect methods estimate soil moisture by developing a functional relationship between the chemical and physical properties of soil moisture and soil matrix [42]. Automated soil moisture measurement techniques have been developed to determine the actual amount of water available to the vegetation and crop. They can be grouped as quantitative and qualitative. The quantitative method includes radiological techniques (such as neutron scattering and gamma-ray attenuation) and soil-water dielectric techniques (such as time-domain and frequency-domain reflectometry). They measure the actual amount of moisture content that is present within the soil layer. The qualitative methods include soil-water potential instrumentation (such as tensiometer, resistance blocks, and psychrometers). These techniques enable repeated measurement of soil moisture at the same location without disturbing the soil layer. To calibrate the automated soil moisture probes, soil bulk density is used. Appendix A provides a detailed review of different methods (direct and indirect) for the measurement of soil moisture with their pros and cons. Table 2 summarises the key characteristics of different in-situ measurement techniques and instruments.

The International Soil Moisture Network (ISMN) was launched in 2009 to provide a seamless database of soil moisture that could be used as ground truth for various applications, such as calibration and validation of satellite-derived soil moisture products, and applications related to hydrology, agronomy, and climate change models [43], [44], [45], [46]. Up till August 2021, about 2800 operating stations have been set up successfully globally [47]. The data recorded at these stations are publicly available. They

TABLE 2. Key characteristics of the in-situ methods and sensors used for soil moisture measurement.

Methods / Sensors		Accuracy and Reliability	Key advantages	Key disadvantages	Cost	Calibration required	Suitable soil	References
Oven dry	**Gravimetric**	High	1. Simple and highly accurate. 2. Direct method 3. Used to calibrate indirect methods.	1. Time consuming and destructive. 2. Labor-intensive. 3. Cannot be automated.	Low	No	All	[48], [49]
	Volumetric	High	1. Simple and highly accurate. 2. Direct method. 3. Used to calibrate indirect methods.	1. Time consuming and destructive. 2. Labor-intensive. 3. Requires bulk density	Low	No	All	[18], [50]
Radiological techniques	**Neutron probe**	Medium	1. Not hindered by environmental factors (*i.e.,* temperature). 2. It is slightly hampered by salinity and chemical composition of the soil.	1. Not recommended for near surface study. Inaccurate for shallow measurements (< 30 cm). 2. Consist of radioactive source (*i.e.,* chances of radiation hazard).	High	Yes	All	[51], [52]
	Gamma rays probe	High	1. Recommended for near surface study. 2. Independent of atmospheric conditions.	1. Labor-intensive 2. Consist of radioactive source (*i.e.,* chances of radiation hazard).	High	Yes	All	[53]
Soil-water dielectric techniques	**TDR**	High	1. Quick response time. 2. Less destructive. 3. Can be automated.	1. Expensive 2. Requires calibration for precise result.	High	Yes	All except saline soil.	[19], [54]
	FDR	High	1. Quick response time. 2. Less destructive. 3. Can be automated.	1. Limited performance under saline or highly conductive heavy clay soils. 2. Requires calibration for precise result.	Medium	Yes	All except saline soil.	[55], [56]
Soil-water potential tecniques	**Tensiometer**	High	1. Can be automated. 2. Not affected by soil salinity.	1. Slow response time. 2. Maintenance issue (*i.e.,* requires frequent maintenance). 3. Limited soil suction range	Low	Yes	All except clayey and silty soils.	[57]
	Resistance block	Medium	1. Can be automated. 2. Recommended for root condition study.	1. Hindered by environmental factors (*i.e.,* temperature). 2. Blocks degrade over time and lose their calibration properties.	Low	Yes	All except sandy soils.	[18], [58]
	Psychrometers	High	1. Re-calibration is not an issue. 2. Portable	1. Difficult to use in a low humid air. 2. Requires periodic maintenance.	Medium	Yes	All	[59]

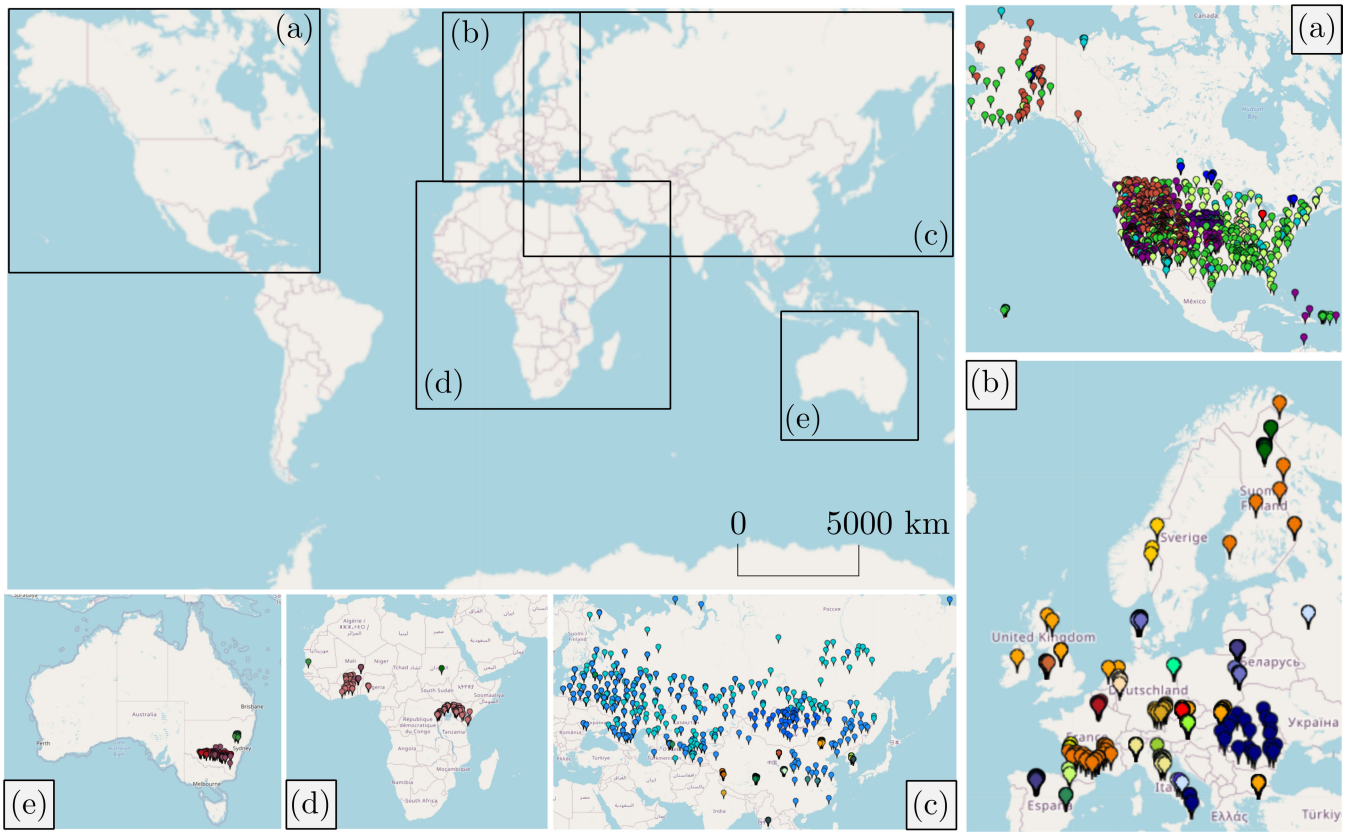

FIGURE 3. Distribution of ground stations (status as of August 2021) for soil moisture measurement across the globe. Rectangles (a-e) show the regions (North America, Europe, Asia, Africa, and Australia, respectively) with the distribution of ground measurement stations.

can be freely downloaded from (https://ismn.geo.tuwien.ac.at/en/data-access/). The spatial distribution of the ground stations (soil moisture) is unevenly distributed globally (Figure 3). For example, one can observe a dense network in the United States and Europe, and only a few stations in Africa, India, and Australia (Figures 3a-e). In these data-scarce regions, one cannot rely only on the ISMN, especially for applications requiring accurate and precise soil moisture measurements.

B. REMOTE SENSING

Recent advancements in satellite and airborne remote sensing have enabled the monitoring of soil moisture at regular intervals at global and regional scales. Remote sensing can be used to acquire images in the optical, thermal, and microwave region of the electromagnetic spectrum. Optical remote sensing uses the radiation energy reflected from the Earth's surface (*i.e.,* surface reflectance) to estimate surface soil moisture. It provides soil moisture at higher spatial resolution [60], [61]. The two widely used techniques in the optical remote sensing of soil moisture are based on the vegetation index, and single spectral analysis [62]. The former uses the difference in vegetation index to estimate the surface soil moisture. The single spectral analysis determines the relationship between soil moisture and surface reflectance by exploiting the difference in the reflectance of the water-absorption and non-absorption bands [63], [64]. Thermal remote sensing uses the radiation energy emitted by the Earth's surface (acquired in the thermal infrared region of the electromagnetic spectrum). The thermal inertia and temperature index are the two widely used methods to estimate soil moisture. In thermal inertia methods, a relationship between thermal inertia and soil moisture is established by determining the change in the soil temperature, whereas the temperature index method uses the land surface temperature to estimate soil moisture. Besides standalone capabilities, optical and thermal remote sensing are often used synergically to estimate surface soil moisture (*i.e.,* triangle, trapezoid, and temporal information-based method) [65], [66], [67], [68], [69]. With its day-night capabilities and being less affected by atmospheric perturbation, microwave remote sensing has emerged as an effective tool in recent years [70]. The soil moisture signal is much stronger in the microwave than in optical or thermal.

The microwave remote sensing can be categorised as active and passive. The passive sensors (*i.e.,* radiometer) detect microwave energy emitted naturally within their field of view, whereas the active microwave sensors (*i.e.,* scatterometer and radar) provide a radiation source to illuminate the object. Both these techniques can sample the surface soil moisture without being seriously impacted by the non-precipitating atmosphere. Kondratyev et al. [80] developed an algorithm

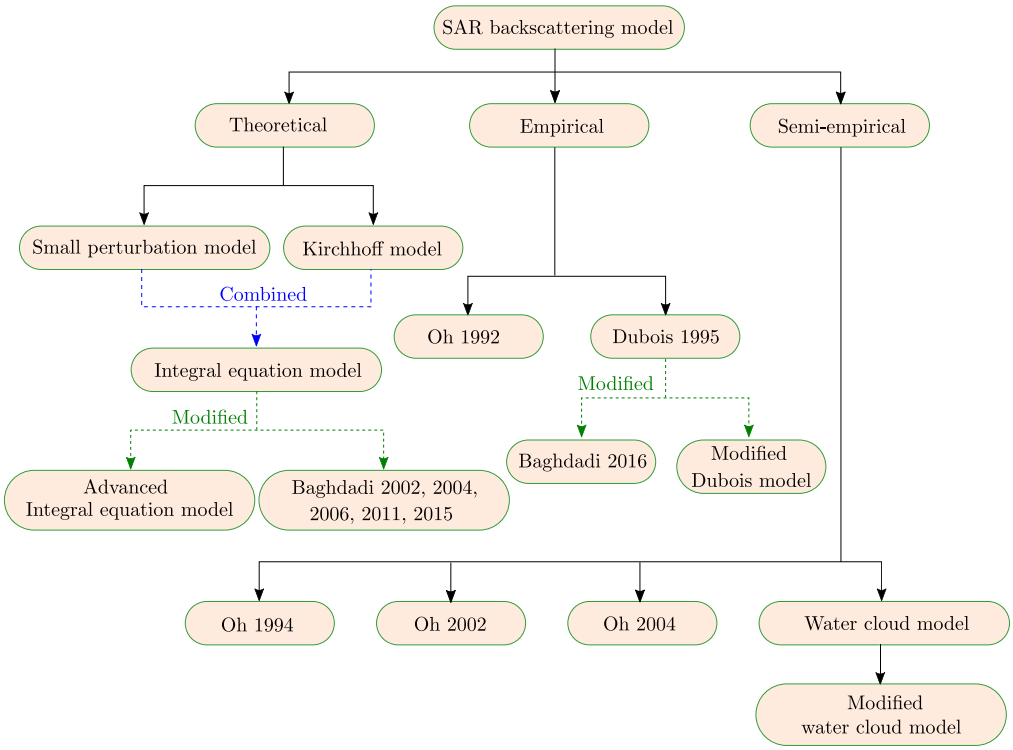

FIGURE 4. Taxonomy of different empirical, semi-empirical, and theoretical models used simulate the radar backscatter.

to estimate soil moisture using passive microwave images. They considered the moisture gradient of each soil type from the emissivity recorded by the radiometer (operating at a wavelength of 18 cm). They found a high variation in the observed and the radiometer-derived soil moisture. Later, Basharinov et al. [81] used a 3 cm radiometer to estimate soil moisture. Their approach could accurately estimate soil moisture over sandy and clayey soils. Later, several experiments have been conducted to improve the accuracy of the soil moisture derived from radiometer [82], [83], [84], [85], [86]. Advanced Microwave Scanning Radiometer for EOS (AMSR-E), launched in May 2002, provides soil moisture (2002-2011) at spatial resolution varying from 5 to 50 km at every 2–3 days interval [87]. Aquarius (L-band) satellite mission (2011-2015) has been used to monitor global soil moisture products of spatial resolution 40 km at every 7 days interval [88], [89], [90]. Passive satellites such as AMSR-2, SMOS, and SMAP are currently operational. They provide global soil moisture products at different spatial and temporal resolutions. For example, the AMSR-2 satellite (launched in May 2012) provides soil moisture at a spatial resolution of 25 km at every 2 days interval [91], [92].

The passive microwave remote sensing soil moisture products usually have a low spatial and high temporal resolution. However, soil moisture estimated from active microwave remote sensing generally has a high spatial and low temporal resolution. The commonly available active remote sensing soil moisture products are scatterometer-derived. ERS Scatterometers *i.e.,* ERS-1 (1991-1996) and ERS-2 (1995-2011) satellites operate at C-band frequency. Magagi and Kerr [93], Pulliainen et al. [94], and Wagner et al. [95] proposed different algorithms to estimate soil moisture (spatial resolution 50 km and revisit time 3-4 days) from the backscatter values of ERS-1/2 satellites. These algorithms have been further applied on Advanced Scatterometer (ASCAT) based satellites such as MetOp-A (from 2006 to 2021), MetOp-B (from 2012 to present), and MetOp-C (from 2018 to present) to estimate daily soil moisture at 25 km spatial resolution. Presently SAR-derived approaches are relatively less developed as compared to the scatterometers in terms of their routine use. However, SAR-based soil moisture products are continuously evolving with the launch of Sentinel-1, and the status is expected to improve with the upcoming NISAR mission.

This review mainly discusses the SAR-based approaches which are frequently used for soil moisture estimation. Different models (empirical, semi-empirical, and theoretical) based on the backscattering mechanism of radar signals have been developed to estimate soil moisture from microwave images (Figure 4). A detailed review of these models is compiled in Appendix B. Table 3 provides a summary of recent studies on estimating soil moisture using backscattering models. We noticed that the Integral Equation Model (IEM) and Water Cloud Model (WCM) had been widely used to estimate soil moisture. The number of publications on soil moisture has

TABLE 3. State-of-the-art studies in soil moisture estimation using different backscatter models.

Publications	In-situ soil moisture	Satellite mission (SAR)	Backscattering model	Performance metrics	Country
[71]	FDR	Gaofen-3 (GF-3)	WCM	R = 0.69 RMSE = 0.05 m^3/m^3	China
[72]	TDR	RADARSAT-2	IEM (calibrated) WCM	R = 0.82 RMSE = 4.15 vol. %	Canada
[73]	Oven dry (Gravimetric)	PALSAR-2	WCM	R = 0.55 to 0.90 RMSE = (0.046 to 0.10) m3m3	Malaysia
[74]	ISMN	Sentinel-1	Oh WCM	R = 0.68 RMSE = 0.08 m^3/m^3	Tibetan Plateau
[75]	COSMOS SMAPVEX12 (Manitoba)	Sentinel-1	Oh WCM	R = 0.69 to 0.82 RMSE = 0.069 m^3/m^3	Canada
[76]	SMAPVEX16 (Manitoba)	Sentinel-1	WCM Advance IEM	R = 0.81 MAE = 0.039 cm^3/cm^3 RMSE = 0.048 cm^3/cm^3	Canada
[41]	TDR Oven dry (Volumetric)	Sentinel-1	Modified Dubois model	R = 0.87 Bias = 0.018 m^3/m^3 RMSE = 0.035 m^3/m^3	India
[77]	TDR	Sentinel-1	Oh model	R = 0.92 Bias = 2.45 vol. % RMSE = 3.19 vol. %	Morocco
			IEM model	R = 0.91 Bias = 0.71 vol. % RMSE = 2.40 vol. %	
[78]	TDR	PALSAR/ALOS-2	WCM Dubois Oh IEM Baghdadi	RMSE = (6.7 - 16.1) vol. %	India
[79]	SMAPVEX12 (Manitoba)	Radarsat-2	WCM	R = 0.59 RMSE = 0.069 m^3/m^3	Canada

increased significantly after the launch of Sentinel-1 satellite missions. Sentinel-1 satellites acquire images only in dual-polarised mode; therefore, the backscatter models developed for the quad-polarised data can not be used for soil moisture estimation. Researchers have modified the backscattering models by reducing the unknown parameter surface roughness, which can be estimated from empirical equations. This enables estimating soil moisture from the dual polarised data. This modification introduces an approximation error into the model [96]. Such limitations can be eliminated with data-driven models.

The data-driven machine learning models require various input features as the training set, based on which the response variable is to be predicted (Figure 5). Previous studies have reported that the microwave backscatter (*i.e.,* VV, VH, HH, and HV), graphical indicators (*i.e.,* NDVI, and NDWI), topography (*i.e.,* elevation), geolocation information (*i.e.,* latitude and longitude) can be used as potential input features to predict soil moisture [97]. These features can be obtained from publicly available remote sensing images and can be used to train appropriate machine learning models to predict soil moisture.

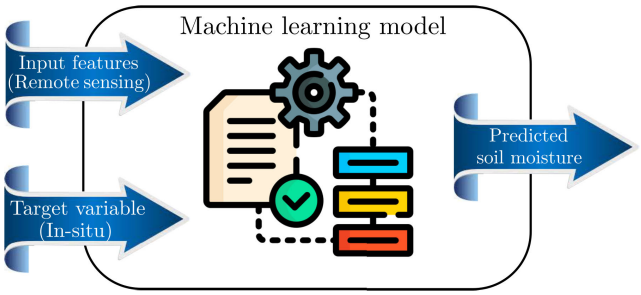

FIGURE 5. Illustration of the interlinkage of machine learning with remote sensing and in-situ observations.

C. SUMMARY AND DISCUSSION

We discussed and summarised the advantages and disadvantages of various techniques that are generally used to measure soil moisture at the local or plot scale. Based on the applications, time constraints, fund availability, and accuracy, appropriate techniques to estimate soil moisture can be applied. We have also reviewed the efficiency of microwave remote sensing images in estimating soil moisture at regional and global scales. We discussed recent studies

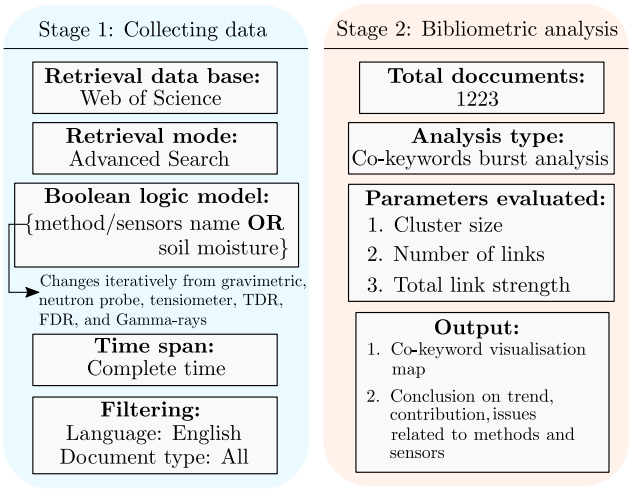

FIGURE 6. Strategy used for the data extraction and details of the bibliometric analysis.

based on backscattering models (empirical, semi-empirical, theoretical) to assess soil moisture. Finally, we have highlighted the potential of machine learning algorithms together with the in-situ measurement and remote sensing images to model and predict soil moisture at different spatial and temporal scales.

III. BIBLIOMETRIC ANALYSIS: IN-SITU

We have performed bibliometric analysis using VOSviewer (Visualisation Of Similarities) software [98]. This publicly available software is used to perform bibliometric analysis on a large number of research manuscripts [99], [100], [101]. We performed this analysis based on the author keywords of 1223 research manuscripts published in the WoS from 1970 to 2022 (till 15th January 2022). We further performed an individual analysis of the more frequently used in-situ soil moisture methods and sensors. We computed the cluster size, the number of links, and the total link strength for gravimetric, neutron probe, tensiometer, TDR, FDR, and Gamma-rays probe.

Any bibliometric maps generated, visualised, analysed in VOSviewer consist of items indicating, according to VOSviewer, a connection or relation between the two items. Each link represents the bibliographic coupling between them (*i.e.,* keywords). We have reported the co-occurrence link between the two items. Each link has a positive strength associated with it. Higher the strength value, the stronger the link. The total link strength corresponds to the number of publications in which the two keywords had occurred together. Both items and the link between them constitute a map. Further, different items are grouped together to form a cluster. A cluster is a set of items present on the map, and each cluster is assigned a number (and different colours). The clusters are formed by using the VOS clustering algorithm [102]. It is a unified algorithm that is widely used for mapping, and bibliometric clustering networks [103]. The search term and strategy for performing this analysis are illustrated in Figure 6.

In stage 1, we downloaded the metadata of 1223 research documents using the advanced search tool from the official site of the WoS (https://www.webofscience.com/wos/woscc/advanced-search). A Boolean logic-based query is passed to search for the relevant documents. The query consists of a method or sensor name followed by a fixed term '*soil moisture*.' We have not placed any filtering in the time and document types except for an English language filter. We fed the downloaded metadata in the VOSviewer to perform co-keyword burst analysis for each method and sensor.

The map for each method and sensor is shown in Figure 7 along with their cluster size, number of links, and the total link strength. We found that the tensiometer emerged with the most number of clusters (*i.e.,* 7), while the TDR appeared with the most number of links (*i.e.,* 460) and had the highest total link strength (*i.e.,* 674). It indicates that the TDR is the most frequently used instrument for soil moisture measurements. The application terms associated with TDR are electrical conductivity, vegetation, drought, and validation. The neutron probe ranked second with a total link strength of 214. The gravimetric method appeared to have the least links (*i.e.,* 86) and the total link strength of (*i.e.,* 104), indicating its less usage in estimating in-situ soil moisture. The frequently appearing application terms considering all methods are field calibration, drought, and electrical conductivity.

A. SUMMARY AND DISCUSSION

Table 4 reports the result of bibliometric analysis. We performed the complete analysis by considering items (*i.e.,* keywords) that occurred at least twice to avoid disconnected maps. The TDR has the highest number of items (*i.e.,* 60). They are grouped into six clusters shown in different colours (Figure 7d). A total of 460 links formed between them, which resulted in a total accumulated link strength of 674. The most frequently used item is "*time-domain reflectometry*". USA emerged as the country with the most publications, which considered TDR for in-situ soil moisture, while Brocca et al. [106] is the most cited publication. FDR has the least number of items that are grouped into five clusters (Figure 7e), having 138 links and 173 total link strength. In the case of FDR, "*moisture*" is the most frequently used item, and Kelleners et al. [107] is the most cited publication.

IV. BIBLIOMETRIC ANALYSIS: APPLICATIONS AND ALGORITHMS

We have performed the bibliometric analysis through the VOSviewer software to find the most frequently linked applications with in-situ soil moisture and machine learning algorithms. We execute a query mentioning the soil moisture sensors with the term application (*i.e.,* {*soil moisture sensor*} *OR* {*application*}) to download the metadata from the web of science database. We then performed co-keywords

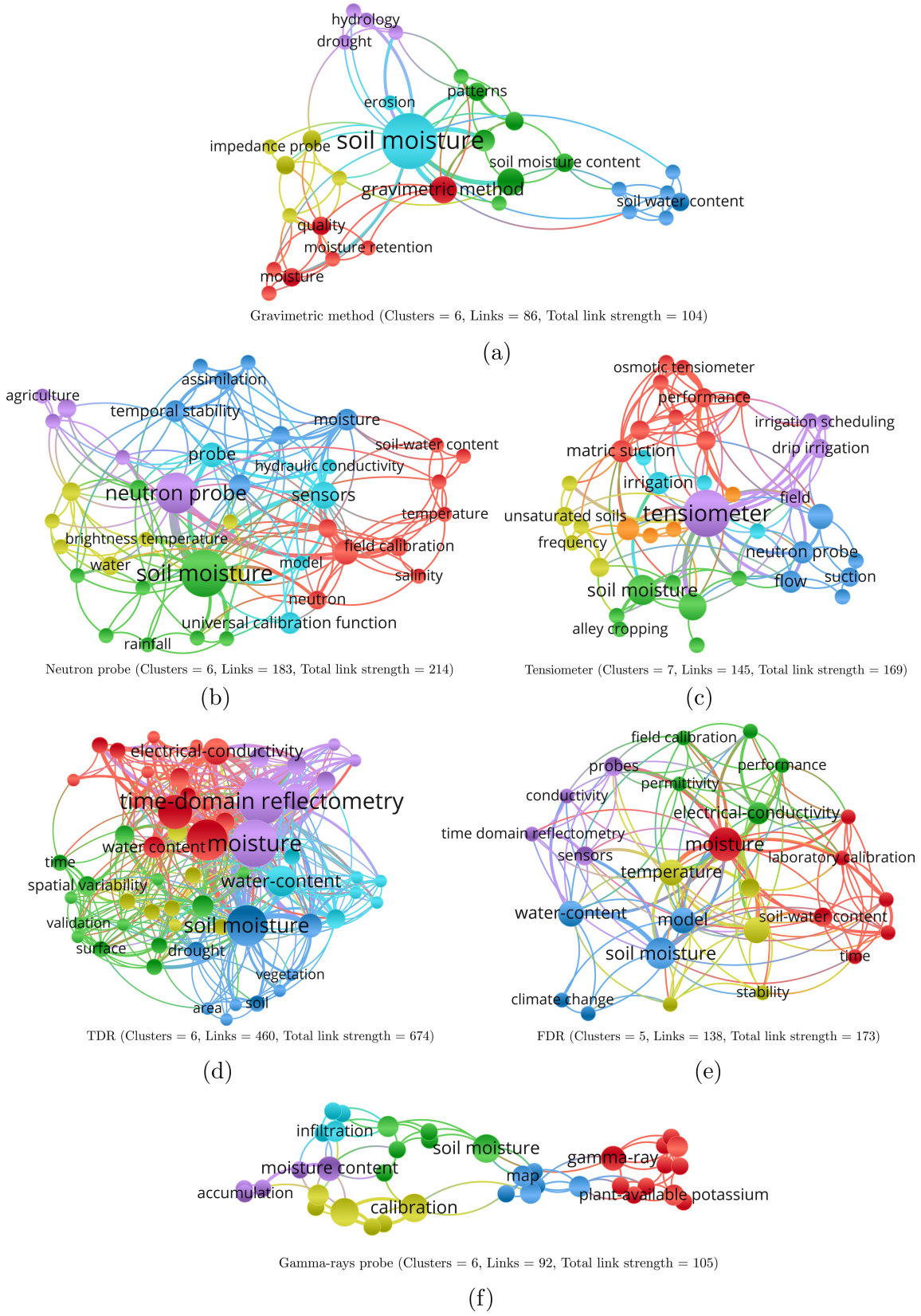

FIGURE 7. Bibliometric analysis of all the prominent in-situ soil moisture measuring methods and sensors. We considered 1223 research manuscripts published in Web of Science from 1970 to 2022 (till 15th January 2022).

TABLE 4. Comparison of the bibliometric analysis for all the prominent soil moisture estimation methods and sensors.

Method/Sensors	Items (with at least two occurrence)	Cluster	Links	Total link strength	Most frequently used keyword	Country with most publications	Most cited publication
Gravimetric	35	6	86	104	soil moisture	USA	[95]
Neutron probe	43	6	183	214	soil moisture	USA	[104]
Tensiometer	40	7	145	169	tensiometer	USA	[105]
TDR	60	6	460	674	time-domain reflectometry	USA	[106]
FDR	26	5	138	173	moisture	USA	[107]
Gamma-ray probe	38	6	92	105	gamma-ray attenuation	Italy	[108]

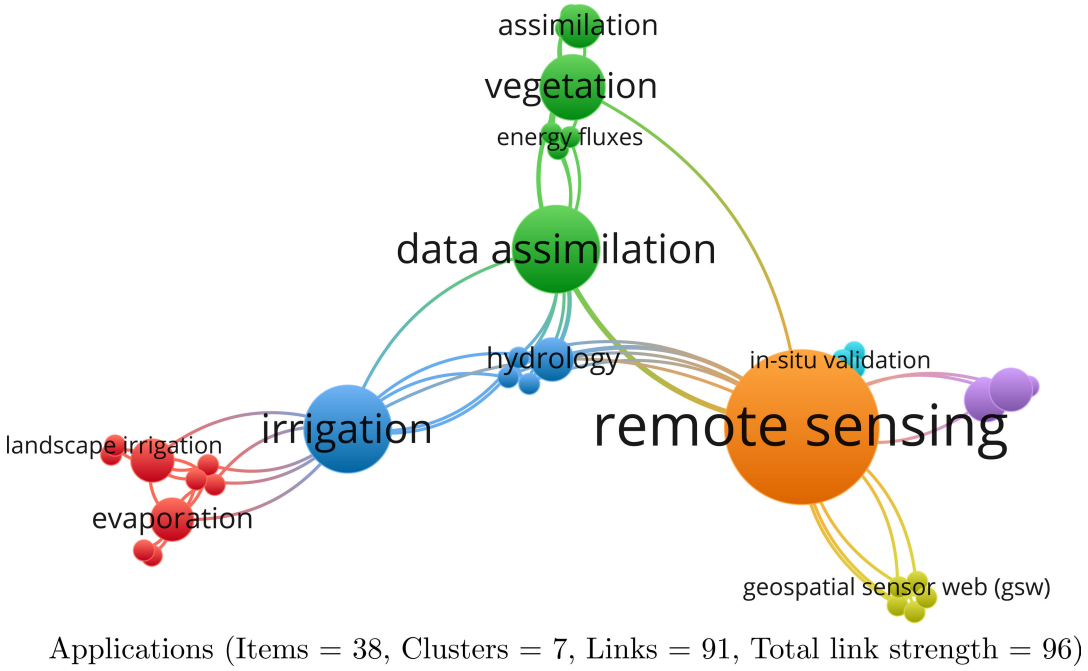

FIGURE 8. Major application areas of in-situ soil moisture methods and sensors. We considered 1060 research documents published from 1991 to 2022 (till 15th January 2022) in the web of science.

burst analysis on 1060 documents to find the application that appeared the most in conjunction with soil moisture sensors and plotted the corresponding results (Figure 8). We found several applications associated with the soil moisture sensors, such as remote sensing, irrigation, control systems, hydrology, agriculture, geospatial sensor web, data assimilation, agriculture, floods, and landscape irrigation. Remote sensing was the most frequent application associated with the study of soil moisture sensors.

We have also executed a query relating soil moisture and machine learning term (*i.e.,* {*soil moisture*} *OR* {*machine learning*}) in the advance search option of the web of science database. We downloaded the metadata and fed it to the VOSviewer software. Subsequently, we performed the co-keyword burst analysis and plotted the corresponding map in Figure 9. Interestingly, random forest, neural network, and support vector machine are the top three machine learning algorithms that have been applied frequently together with in-situ soil moisture measurement. The other algorithms are Gaussian process regression, decision tree, automated machine learning, deep belief network, fuzzy logic system, and extreme machine learning.

In the upcoming subsections, we elaborate the top three machine learning algorithms (*i.e.,* random forest, neural network, and support vector machine) from a regression point of view. Finally, we summarise the recent research article that uses machine learning algorithms, in-situ measured soil moisture, and remote sensing images to predict the soil moisture in Table 5. We highlight the in-situ measurement technique, remote sensing datasets, and the corresponding satellite mission, the machine learning algorithms, the best-performing algorithms, along with the corresponding performance metrics, and the study area.

A. RANDOM FOREST

Random forest regression is a supervised technique that uses ensemble learning for regression. The random forest classifier creates several decision trees through the bagging method during the training phase by optimising the tuning parameters. According to Breiman [109], the default value of the tuning parameters for the regression problem is 200 trees and p/3 number of features in each split. However, the optimal tuning parameter selection depends on the problem, as the

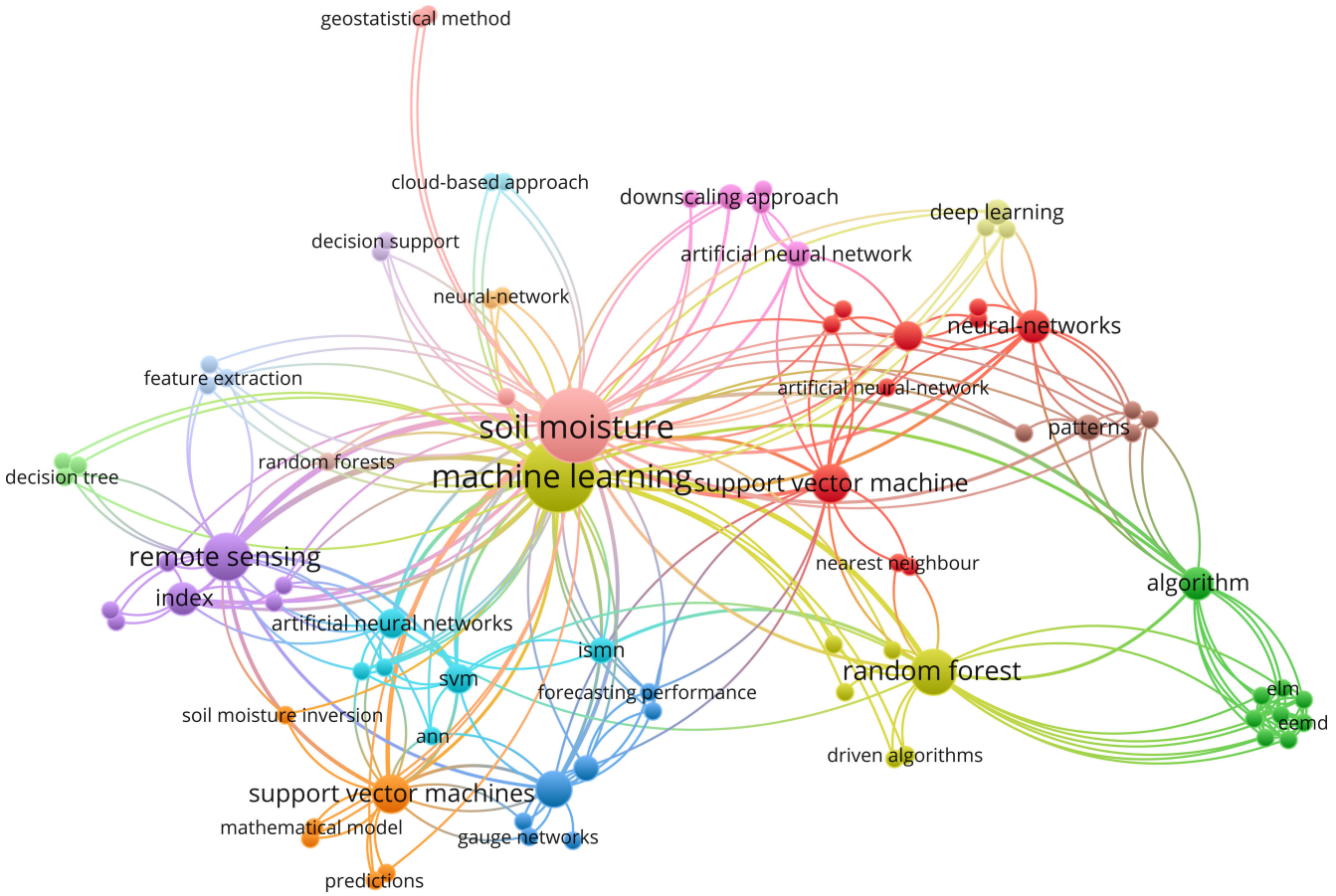

FIGURE 9. Machine learning algorithms used for soil moisture retrieval. We considered 512 research documents published from 1995 to 2022 (till 15th January 2022) in the web of science.

default values may not give promising results [110]. Once the model is trained, we feed the testing data into the input of the trained trees. The prediction from each decision tree is averaged to obtain the final value (Figure 10).

B. NEURAL NETWORK

Neural networks (also known as ANN) are a network of artificial neurons. For regression-based problems (such as soil moisture estimation), we generally use a feed-forward neural network [111], [112]. Figure 11 illustrates a typical structure of a general feed-forward ANN. It consists of an input, hidden, and output layer. The input layer consists of the input features, while the hidden layer consists of several neurons that collect the weighted input from the previous layer. The output layer consists of a response variable. A bias term is linked to each neuron present in the hidden layers. Further, each layer is followed by an activation function. The role of the activation function is to decide whether a particular neuron should be activated or not. It applies a non-linear transformation at the neuron's output to make it capable of solving complex problems [113]. In general, a linear transformation (*i.e.,* purelin) is used at the input and the output layer, while a hyperbolic tangent sigmoid transfer function (*i.e.,* tansig) is used at each hidden layer [114], [115]. In feed-forward ANN, the neurons of one layer are connected to the neurons of the successive layers, hence do not form any loop.

To train the feed-forward ANN efficiently, back-propagation algorithms are widely used. It performs iterative calculations to determine the optimal weights and bias by optimising the error function [116]. Readers may refer [117], [118] to know details on feed-forward ANN.

C. SUPPORT VECTOR MACHINE

Vapnik [119] introduced the most notable classification algorithm (*i.e.,* support vector machine) to the nature of statistical learning theory (Figure 12). Later, Drucker et al. [120] modified it to deal with a regression problem known as support vector machine regression or support vector regression. The response variable, $y(x)$, can be estimated by using the following equation;

$$y(x) = \sum_{i=1}^{N} (\alpha_i - \alpha_i^*) K(x_i, x_j) + b \tag{1}$$

TABLE 5. Summary of the recent state-of-the-art studies in soil moisture estimation using remote sensing and machine learning algorithms.

Publication	Soil moisture datasets	Remote sensing datasets	Satellite missions	Machine learning algorithms	Best performing algorithm	Performance metrics	Country (Study area)
[133]	TDR	1. Reflectance (NDVI) 2. Backscatter (VV, VH) 3. Others (incidence angle, DEM)	Sentinel-1/2	ANN, GRNN, RBN Exact RBN, GPR SVR, RF, RNN, AutoML Boosting EL, BDT	ANN	RMSE (0.04 m^3/m^3) R = 0.80	India
[134]	TDR	1. Reflectance (NTR and NDVI)	UAV	Automated machine learning model	Automated machine learning model	RMSE (0.04 cm^3/cm^3) NS (>0.9)	USA
[135]	TDR	1.Backscatter (VV and VH)	Sentinel-1	ANN, RF, SVM RBF, WM, SBC ANFIS, HyFIS, DENFIS	SBC	R (0.64) RMSE (0.075 m^3/m^3) Bias (-0.009 m^3/m^3)	India
[112]	TDR Oven dry	1. Reflectance (NDWI) 2. Backscatter (VV and VH)	Sentinel-1 Landsat 7 and 8	ANN LRM	ANN	RMSE (0.035 cm^3/cm^3) Bias (-0.024 cm^3/cm^3) R (0.73)	Ethiopia
[136]	TDR	1. Reflectance (LST, NDVI, Albedo) 2. Others (DEM, Latitude, Longitude)	MODIS	GRNN	GRNN	RMSE (0.069 cm^3/cm^3) Bias (0.003 cm^3/cm^3) ubRMSE (0.069 cm^3/cm^3)	Tibetan Plateau
[137]	TDR	1. Reflectance (LST, Blue, Green, Red, NIR, SWIR1 SWIR2)	Landsat 8	ANN, RF SVM, EN	RF	NS (0.73)	Iran
[138]	ISMN	1. Reflectance (VWC and NDVI) 2. Others (Reflectivity, TES, LES Incidence angle, Elevation, Slope)	CYGNSS MODIS	ANN, RF SVM	RF	R (0.90) RMSE (0.049 cm^3/cm^3) ubRMSE (0.049 cm^3/cm^3)	USA
[139]	TDR	1. Reflectance (Green, Red, NIR)	UAV	ANN, RF SVM, RVR BRT	BRT	R^2 (0.71) MAE (3.78 %)	USA
[140]	TDR	1. Backscatter (HH, HV, VV) Compact Polarimetry	Radarsat-2	ANN	ANN	R (0.7-0.9) RMSE (3-7%)	Canada
[141]	Oven dry	1. Reflectance (Hyperspectral bands)	UAV	RF, ELM	RF	R^2 (0.91) RMSE (1.48%) RPD (3.396%)	China
[142]	TDR	1. Backscatter (VV and VH) 2. Others (Incidence angle)	Sentinel-1	RF	RF	R^2 (0.86) RMSE (3%)	New Zealand

Note: Binary decision tree (BDT), Random forest (RF), Support vector machine (SVM), Artificial neural network (ANN), Elastic net regression (EN), Nash–Sutcliffe efficiency (NS) NASA's Cyclone GNSS (CYGNSS), Unbiased RMSE (ubRMSE), Vegetation water content (VWC), Slope of the trailing edge of the reflectivity (TES) Leading edge slope of the reflectivity (LES), Relevance vector regression (RVR), Boosted regression trees (BRT), Mean absolute error (MAE), Vertical-Vertical (VV) Vertical-Horizontal (VH) backscatter, Radial basis function (RBF), Wang and Mendel's (WM), Subtractive clustering (SBC), Adaptive neuro-fuzzy inference system (ANFIS) Hybrid fuzzy interference system (HyFIS), Dynamic evolving neural fuzzy inference system (DENFIS), Extreme learning machine (ELM), relative percent deviation (RPD) Generalised regression neural network (GRNN), Land surface temperature (LST), Normalised difference water index (NDWI), Linear regression model (LRM) Near-infrared transformed reflectance (NTR), Normalized difference vegetation index (NDVI), Radial basis network (RBN), Gaussian process regression (GPR)

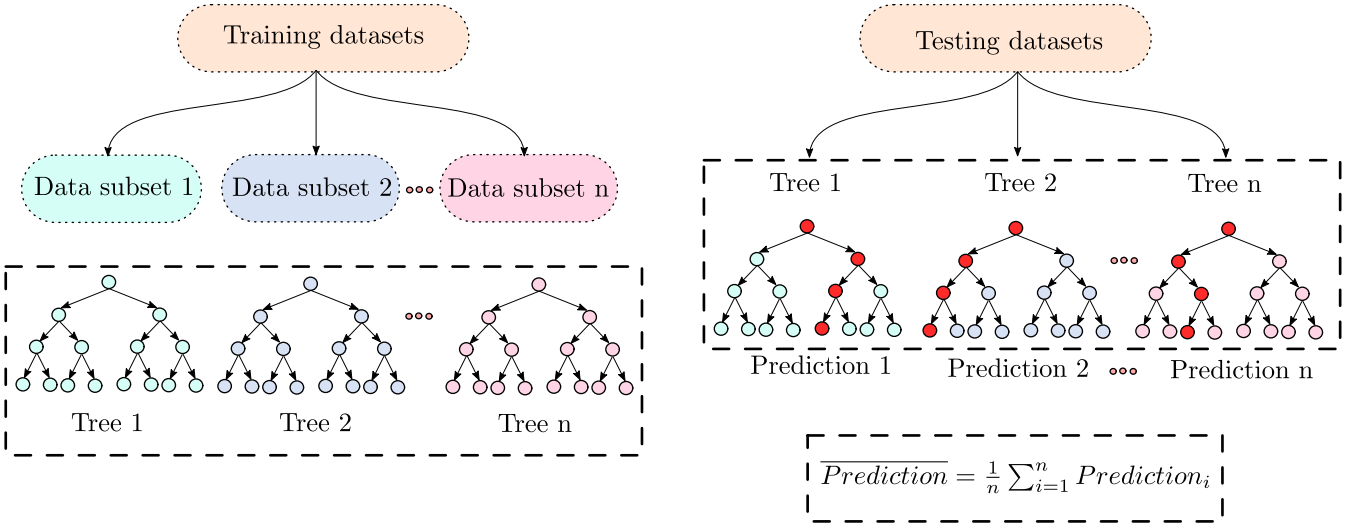

FIGURE 10. Illustration of the training and prediction of random forest regression algorithm.

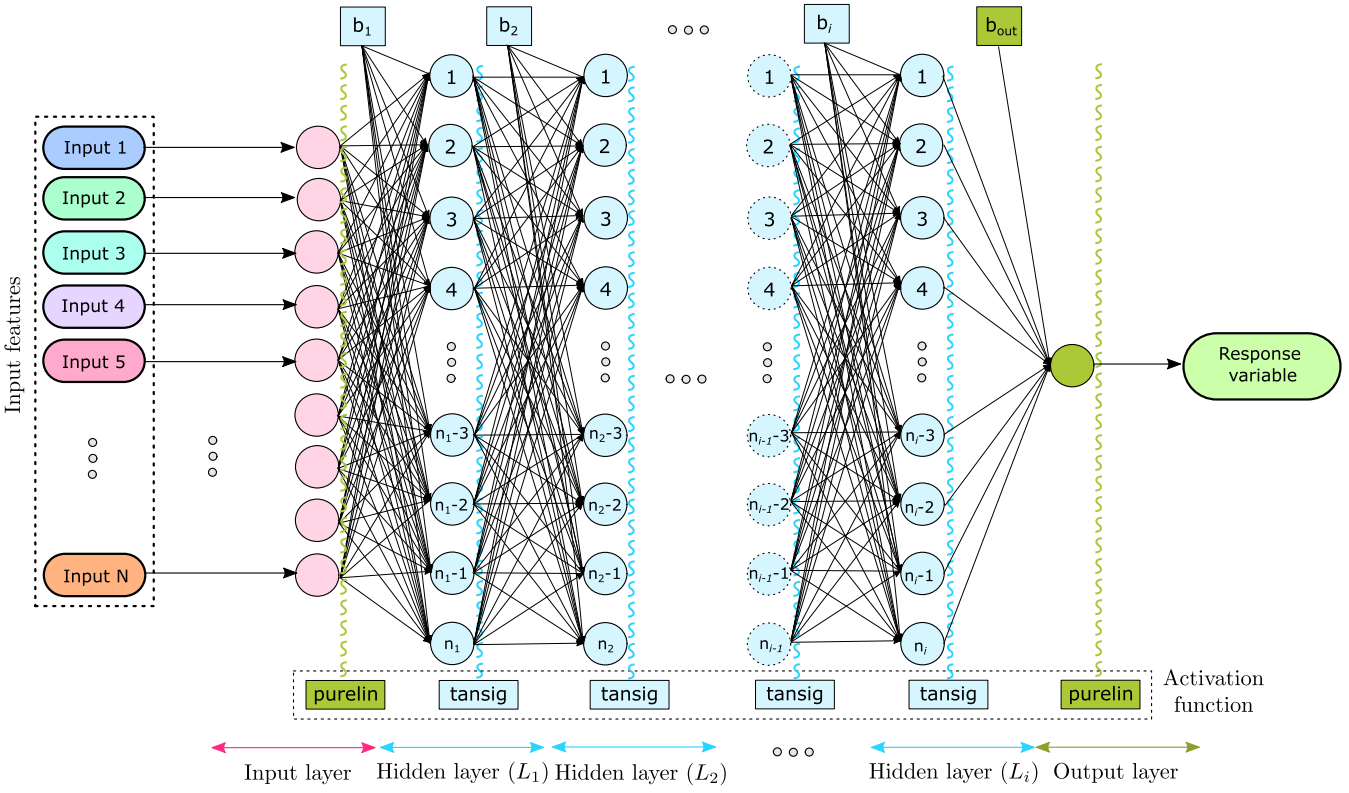

FIGURE 11. Illustration of the general architecture of a fully connected feed-forward ANN.

where $K(x_i, x_j)$ is the kernel function, and b is the bias term. α_i and α_i^* are the Lagrange multipliers. It has an excellent generalisation capability and is widely used in different remote sensing applications [121], [122], [123], [124], [125], [126], [127], [128], [129]. A detailed study about support vector regression can be found in literature [130], [131], [132].

D. SUMMARY AND DISCUSSION

Regression-based machine learning algorithms are used to predict soil moisture. Bibliometric analysis confirms that the random forest, neural network, and support vector machine are the frequently used machine learning algorithms for soil moisture prediction (Table 6). The performance of these algorithms completely depends on the quality and relevance

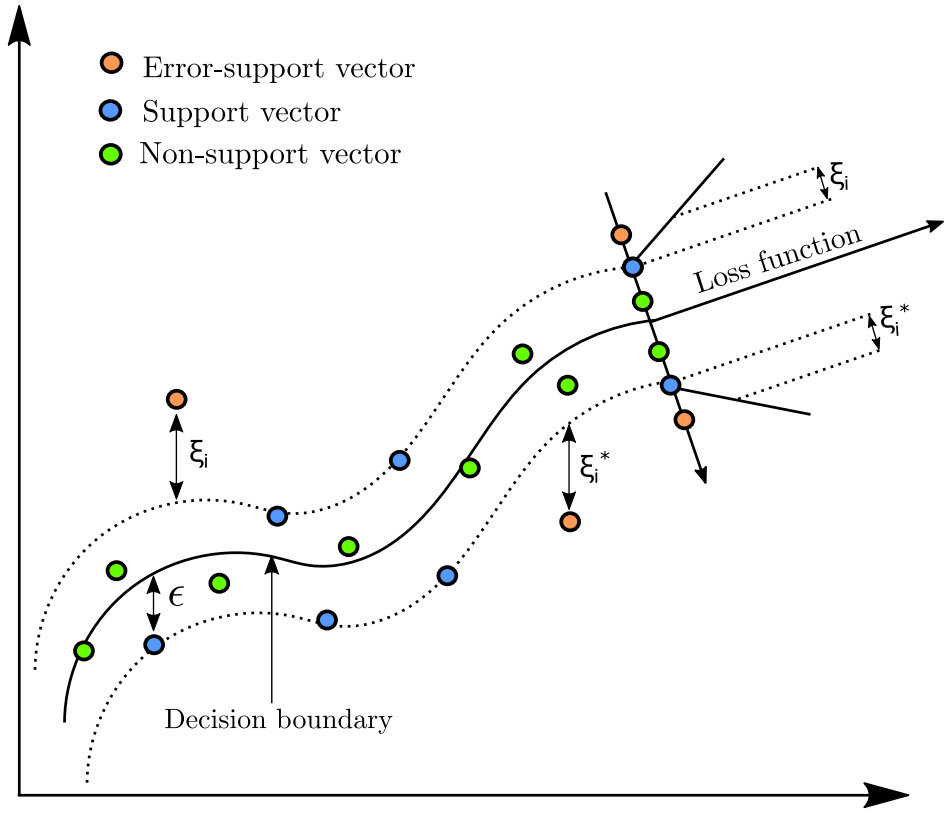

FIGURE 12. Illustration of the working of support vector machine regression.

TABLE 6. Comparison of the bibliometric analysis for the frequently used machine learning algorithms for soil moisture prediction.

Algorithms	Soil moisture problem	Items (with at least single occurrence)	Clusters	Links	Total link strength	Country with most publication	Organisation with most publications	Most cited publication
Random Forest	Regression-based	387	21	3968	4348	China	Chinese Academy of Sciences	[143]
Neural Network	Regression-based	319	19	3104	3400	China	Chinese Academy of Sciences	[111]
SVM	Regression-based	377	18	3872	4208	China	Chinese Academy of Sciences	[111]

TABLE 7. Comparison of the different machine learning algorithms for soil moisture estimation from remote sensing images (predictors) and in-situ soil moisture (response variable).

Performance metrics	Frequently used algorithms			Other benchmark algorithms						
	RF	ANN	SVR	RNN	BDT	GAM	LR	GPR	GRNN	Logistic regression
R	0.20	0.80	0.23	0.17	0.10	0.12	0.32	0.40	0.36	0.30
RMSE [m^3/m^3]	0.06	0.06	0.06	0.08	0.09	0.10	0.07	0.06	0.06	0.06
Bias [m^3/m^3]	0.04	-0.01	-0.08	-0.11	0.03	0.05	-0.01	0.05	0.04	0.01
Note: Recurrent Neural Network (RNN), Binary Decision Tree (BDT), Generalized Additive Model (GAM), Linear Regression (LR), Gaussian Process Regression (GPR), Generalised Regression Neural Network (GRNN).										

of the selected input features. The input feature must contain information about the target variable. All the relevant features that explain the physics of soil moisture must be selected. However, a balance between the number of features and observations must be kept, considering that many input features, although relevant, may degrade the performance of the machine learning model [144]. Selecting the appropriate and relevant input features is more important than selecting a machine learning model.

We found that random forest is the most widely used machine learning algorithm concerning soil moisture estimation (with 387 items, 21 clusters, 3968 links, and 4348 total link strength). China emerged as the country with the most publications for soil moisture prediction using machine learning and remote sensing images. More specifically Chinese Academy of Sciences has appeared as the organisation with the most publications. Some of the most cited publications concerning

soil moisture and machine learning are Im et al. [143], and Ahmad et al. [111].

V. COMPARISON OF MACHINE LEARNING ALGORITHMS

Table 5 reports a comparison of studies conducted in the different study areas, input features, and source of in-situ measurements. For a fair and unbiased comparison, we must evaluate the performance of different machine learning algorithms with the same datasets. We have used the in-situ soil moisture datasets provided by Singh et al. [96]. Using a calibrated TDR, they measured in-situ soil moisture at 78 different locations on the Kosi river alluvial fan of the Himalayan Foreland. We used the in-situ measured soil moisture as the response variable and extracted nine input features from Sentinel-1 and Sentinel-2 satellite images and the digital elevation model of the Shuttle Radar Topographic Mission (SRTM). Total five input features (*i.e.,* VV, VH, VH/VV, VH-VV, local incidence angle) from Sentinel-1, one (*i.e.,* NDVI) from Sentinel-2, and three features (*i.e.,* elevation, latitude, and longitude) from SRTM have been selected.

The entire datasets are divided into training (*i.e.,* 60%) and testing (40%). The training data has been used to train ten benchmark algorithms: RF, ANN, SVR, RNN, BDT, GAM, LR, GPR, GRNN, and logistic regression. Bayesian optimisation has been used to tune the hyperparameters of the machine learning models [145]. Once we trained the models, we used the testing data to evaluate the algorithms' performance. We use R, RMSE, and bias as the performance metrics (Table 7). Among all these algorithms, ANN outperforms all the other algorithms with $R = 0.80$, $RMSE = 0.06\ m^3/m^3$, and $bias = 0.04\ m^3/m^3$.

VI. DISCUSSION

In-situ soil moisture measurements are majorly used for calibrating and validating satellite-derived soil moisture and land surface models [43]. This study explores some interesting insights starting from the local scale in-situ soil moisture measurements to the global scale satellite-derived soil moisture, which are discussed in the following subsections.

A. IN-SITU SOIL MOISTURE

We comprehensively reviewed methods and sensors widely used to collect (or measure) in-situ soil moisture. We summarised the key features (*i.e.,* accuracy, reliability, advantages, disadvantages, cost, calibration, and suitable soils) of these methods in Table 2. Depending on the requirements and constraints, one can use different techniques. For example, to measure precise soil moisture values, the conventional approach can be used, whereas if fast and precise measurement is needed, TDR should be used. Before inserting it in the ground, TDR needs to be calibrated for optimal performance, which is time-consuming. Also, the cost associated with TDR is high. For a low-cost solution, Tensiometer can be used for fast and precise soil moisture. Although, it is not recommended for dry soils, and more specifically, for finer texture soils such as clays because of their high water-holding capability. Hence, a proper balance between accuracy, cost, and time must be kept depending on the requirements. Further, for long-term continuous in-situ measurements to analyse the trends in the water cycle worldwide, the harmonised data from ISMN can be used. The only limitation associated with ISMN is the non-uniform distribution of the networks worldwide.

We performed the bibliometric co-keywords burst analysis on the frequently used methods and sensors. To do so, we considered 1223 research publications from the web of science database. The results demonstrate that TDR is refereed in most publications concerning in-situ soil moisture, indicating it to be the most frequently used soil moisture sensor for in-situ measurements. This is probably because of its very precise and fast measurements post calibration [146], [147]. We have summarised the key findings of the bibliometric analysis in Table 4. The most cited publications for each method are gravimetric [95], neutron probe [104], tensiometer [105], TDR [106], FDR [107], and Gamma-ray probe [108]. Remote sensing is the most common application linked with soil moisture sensors. This primarily includes assessing the satellite-derived soil moisture product through direct point-to-pixel comparison [148], [149].

B. SATELLITE SOIL MOISTURE

Microwave remote sensing is considered the most preferred technique for soil moisture observation [150], [151]. Due to the lack of availability of quad-polarised images in the public domain [41], [152], [153], the use of the data-driven model to estimate surface soil moisture has increased exponentially (Figure 1). Random forest, neural network, and support vector machine are the widely used algorithms for predicting soil moisture (Figure 9). These regression-based algorithms map various satellite-derived features (topographic information (*i.e.,* DEM), SAR backscatter, graphical indicator (such as NDVI), optical reflectance, etc.) with the in-situ soil moisture. Further, a new synthetic feature can be created through a linear data fusion of the existing input features [132]. Since all the input features have different units and magnitudes, they must be brought to the same level through various scaling algorithms, such as zscore, min-max, scale, and center mean scaling. If scaling is not performed, the feature having a higher magnitude will govern the machine learning model and produce a biased result [154], [155]. After the feature pre-processing, they are randomly split into the training and testing datasets. The split ratio can be 60:40 (training 60% and testing 40%) or 70:30 (training 70% and testing 30%) or 80:20 (training 80% and testing 20%) depending upon the number of observations [155], [156], [157]. At least 30 observations on the testing data are needed for the results to be statistically significant. The training features and the corresponding in-situ soil moisture can be directly used to

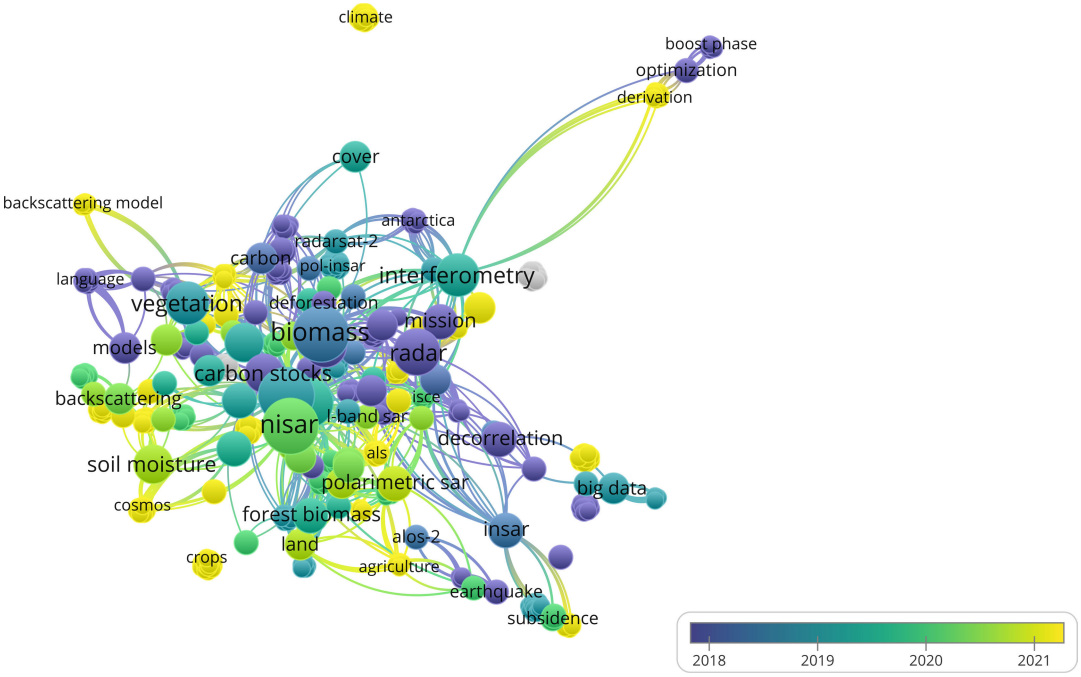

FIGURE 13. Co-keywords analysis of the term NISAR mission. A total of 71 research publications have been considered from the web of science database. The map has 19 clusters, 3326 links, and 281.5 total link strength.

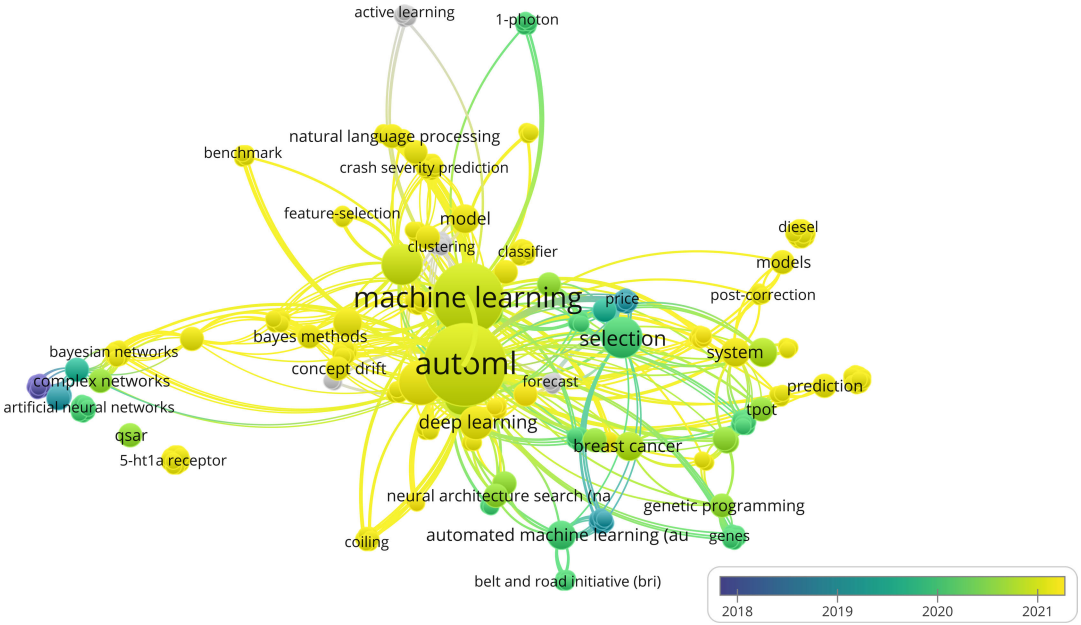

FIGURE 14. Co-keywords analysis of the term AutoML (automated machine learning model). A total of 185 research publications have been considered from the web of science database. The map has 22 clusters, 1562 links, and 184.5 total link strength.

train the machine learning model, which the testing data can validate.

C. FUTURE WORK

As mentioned earlier, the SAR images have high sensitivity towards soil's dielectric property and are more frequently used for soil moisture estimation at a regional and global scale. The majority of the available SAR satellite missions provide only dual polarised backscatter images. The upcoming NASA-ISRO Synthetic Aperture Radar (NISAR) satellite mission will provide quad-polarised images in the public domain. It is the first of its kind in which dual-band (*i.e.*, L- and S-band) data will be acquired within the same mission. It is a joint venture between NASA and the Indian Space Research Organisation (ISRO). NASA is developing the L-band SAR that will operate at a wavelength of 24 cm, and

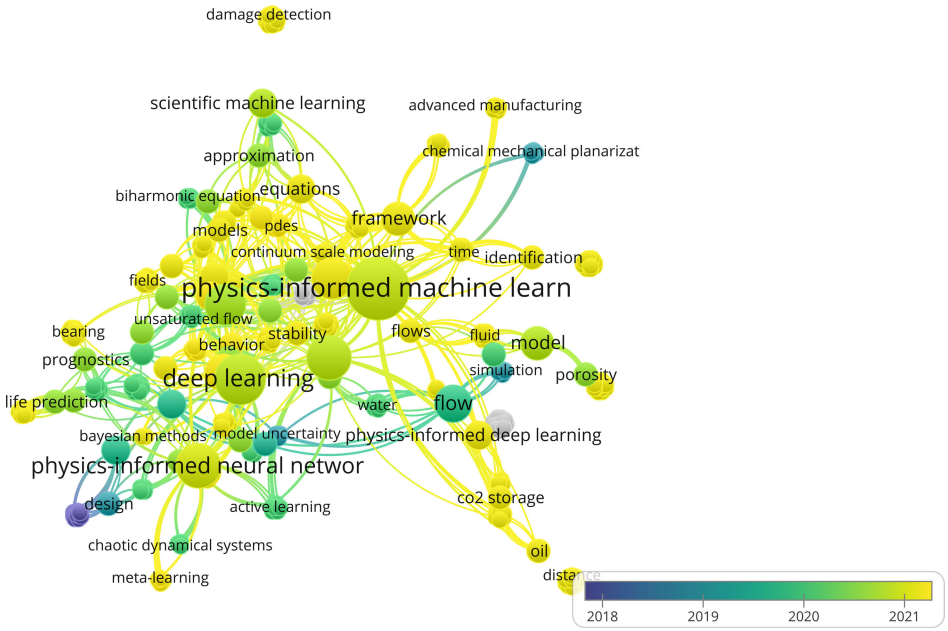

FIGURE 15. Co-keywords analysis of the term physics-informed machine learning. A total of 412 research publications have been considered from the web of science database. The map has 21 clusters, 1817 links, and 203.5 total link strength.

ISRO is developing the S-band SAR that will operate at a wavelength of 9 cm. The mission is expected to be operational in early 2024 (*i.e.,* January 2024). The synergic use of L- and S-band quad-polarised images will improve the quality of the existing soil moisture retrieval process. A co-keywords bibliometric analysis of the term NISAR mission is shown in Figure 13.

Recent developments in the machine learning community can also improve the quality of satellite-derived soil moisture. For example, the use of automated machine learning and physics-informed machine learning has increased recently. Both these algorithms have great potential to excel in the field of remote sensing of soil moisture. AutoML is mainly used to solve real-world problems where the complete process is automated, starting from feature engineering to selecting the best machine learning algorithm [145]. Various types of cloud-based platforms are available to execute AutoML, such as H2O.ai, Google Cloud AutoML, Microsoft Azure AutoML, TPOT (Tree-based Pipeline Optimisation Tool), and many more [158]. To better understand the increasing popularity of AutoML, we performed the co-keywords bibliometric analysis and plotted the map indicating the metrics for the last three years (Figure 14). Another state-of-the-art machine learning algorithm is the physics-informed machine learning [159]. It integrates the data-driven model with the physics associated with the concern problem. The main objective of physics-informed machine learning is to modify the error function or loss function involved in the optimisation process. The traditional loss function (*i.e.,* either MSE or RMSE) is replaced by a modified function that incorporates the general governing physics of the problem. We have also performed the co-keywords bibliometric analysis of the term physics-informed machine learning for the last three years (Figure 15).

Hence, the concurrent use of accurate in-situ soil moisture measurements and the upcoming satellite missions in conjunction with the latest development in the machine learning community will be helpful in improving the accuracy, spatial resolution, and temporal resolution of the satellite-derived soil moisture products.

D. LIMITATIONS

Although we have explored some of the crucial results concerning soil moisture estimation, this study has some limitations. First, we have only considered the data from the web of science database to perform the bibliometric analysis, which considers research publications written in English. This leads to underestimating potential researchers using their vernacular languages to write research manuscripts. Further, the research publications published in new journals are not considered as these journals usually take a few years to get indexed in the web of science database. In addition, we have not considered research manuscripts that are in the public domain as a preprint. In this contribution, we have only reviewed the SAR-based remote sensing approaches for soil moisture estimation among all available remote sensing approaches.

VII. CONCLUSION

The use of soil moisture information coupled with machine learning algorithms has created a new era in the field of hydrology, climate change studies, and agriculture.

The significant increase in the computation facilities has encouraged the use of big data (*i.e.,* remote sensing images) for estimating soil moisture information at the global and regional scale. Developing an efficient machine learning model for global and regional soil moisture prediction requires potential features from remote sensing imagery and accurate in-situ soil moisture information. In this paper, we presented a comprehensive review of the methods and sensors for accurate in-situ soil moisture measurements. We also demonstrated the performance of ten machine learning models for soil moisture estimation considering satellite-derived input features.

The bibliometric analysis of all the frequently used in-situ soil moisture methods and sensors confirms that the TDR is the most frequently used sensor for measuring in-situ soil moisture. Remote sensing is the most likely application for soil moisture sensors. Simultaneously, we also looked for the top machine learning algorithms used in conjunction with in-situ soil moisture. Surprisingly, we found random forest, neural network, and support vector machines as the most used machine learning algorithms. Lastly, we elaborated on these algorithms and presented the recent state-of-the-art studies that presented global or regional soil moisture information by using machine learning, remote sensing, and in-situ soil moisture information. This review will help researchers to effectively select the frequently used in-situ soil moisture estimation method and the best-performing machine learning algorithms for global and regional soil moisture using remote sensing images.

APPENDIX A IN-SITU SOIL MOISTURE METHODS AND SENSORS

This section discusses the strength and weaknesses of the conventional oven drying method and different variants of automated techniques to quantify surface soil moisture. This review highlights the challenges, future opportunities, and application of these methods.

A. OVEN DRY: GRAVIMETRIC AND VOLUMETRIC SOIL MOISTURE

Over the past several years, the gravimetric method for soil moisture estimation has been regarded as the most reliable and robust method. Gravimetric soil moisture, m_g, is defined as the ratio of the mass of the water in the soil sample to the mass of the dry soil. It is expressed in [kg/kg]; however, for the comparative study in the earth sciences, it is usually expressed in percentage. Mathematically m_g is defined as

$$m_g = \frac{m_{water}}{m_{soil}} = \frac{m_{wet} - m_{dry}}{m_{dry}} \tag{A.1}$$

where m_{water} is the mass of the water in the soil sample, expressed as the difference between the weight of the soil sample before drying, m_{wet}, and after drying, m_{dry}. m_{soil} & m_{dry} is the mass of the dried soil. Firstly, 50 g of soil sample is collected from the field with minimum disturbance of the soil structure [42]. Then the collected soil sample is immediately placed in a pre-weighed container. As the container will be placed in an oven, it should withstand high temperatures. An aluminum can is commonly used in the laboratory for electrified heated oven drying. However, non-metallic containers are preferred over aluminum cans if the samples are to be dried in a microwave oven, as microwaves are impenetrable to the metallic cans, which can result in an electrical short circuit. If the collected soil samples are to be transported for a considerable distance, then sterile zip-seal sampling bags should be used to avoid moisture loss from evaporation. The standard drying procedure of the sample involves putting the sample container in an electrified heated oven at a temperature 105°C until the mass gets stabilised to a constant value over a time interval of 24 hours [48], [160].

Due to excessive oxidation at 105°C, a loss of organic matter in the sample occurs, which can be minimised by reducing the temperature from 105°C to 70°C. Hence, a trade-off exists between the temperature and the loss of organic matter from the sample. Doing so will affect the accuracy of the actual moisture content. However, nowadays, microwave ovens are used to rapidly determine the moisture content of organic and organo-mineral soils instead of electrified heated ovens. Although microwave ovens provide a faster estimation of the moisture content, while the organic matter loss is comparable to that of electrified heated ovens [161].

Volumetric soil moisture, m_v, is more meaningful than gravimetric soil moisture as it considers the soil's bulk density and porosity. It is defined as the ratio of the volume of the liquid water, V_{water}, to the volume of the soil, V_{soil}. Usually, m_v is expressed in percentage, but contemporary hydrological communities are adopting m_v in $[m^3/m^3]$. Mathematically, m_v is defined as;

$$m_v = \frac{V_{water}}{V_{soil}} \tag{A.2}$$

Equation A.2, can be extended to get a relationship between m_v and m_g

$$m_v = \frac{m_{water}/\rho_{water}}{m_{soil}/\rho_{soil}} = m_g * \frac{\rho_{soil}}{\rho_{water}} \tag{A.3}$$

where ρ_{soil} is the soil bulk density, ρ_{water} is the water density. Both ρ_{soil} and ρ_{water} are expressed in $[g/cm^3]$. Since the density of water is about 1 g/cm^3, so Equation A.3 can be reduced to;

$$m_v \approx m_g * \rho_{soil} \tag{A.4}$$

If the soil sample contains a substantial amount of stone or gravel, the accuracy of the estimated soil moisture content can be affected, as the stones that are present in the sample contribute directly to the mass measurement of the sample without contributing equally towards the soil porosity. To avoid the effect of stones, Klute et al. proposed the following equation;

$$m_v = m_g * \left(\frac{\rho_{soil}}{\rho_{water}}\right) * \left(1 + \frac{M_{stones}}{M_{fines}}\right) \tag{A.5}$$

where M_{stones} and M_{fines} respectively represent the masses of the stone and fine soil fraction present in the collected soil sample.

Although the microwave oven has decreased the time required for oven drying, it is still a time-consuming and destructive method when compared to automated techniques. These limitations imply that we cannot use this method to measure soil moisture repeatedly over the same location. In spite of its limitations, this method is a benchmark for the calibration process for automated soil moisture measurement techniques.

B. RADIOLOGICAL TECHNIQUES: NEUTRON PROBE AND GAMMA RAYS PROBE

The neutron probe is widely used to measure volumetric soil moisture in a larger sphere. In contrast, the gamma-ray probe measures the soil moisture (volumetric) in a thin layer. Both these methods use portable equipment and can provide multiple measurements of soil moisture at a point of interest after calibration. The neutron probe is the first automatic technique that indirectly measures the volumetric moisture of the soil samples. This microprocessor-based device became popular during the 1950's [162]. It consists of two components: (i) a probe with a shield cover and (ii) an electronic counting system (Figure 16). Both the components are connected via an electric cable [163]. The required depth is measured by lowering the probe into an access tube. The working principle of this probe is based on the interaction of high-energy neutrons with the nuclei of hydrogen atoms beneath the soil surface. A radioactive source emits high-energy neutrons, which after emission, get slow after several elastic collisions with the hydrogen atoms' nuclei. This retardation process is known as thermalisation. Since the element Beryllium has the highest neutron count, it is used exclusively as the radioactive source [164].

The hydrogen atom has nearly the same mass as a neutron and is ten times more capable of slowing down neutrons upon collision than other nuclei. Also, the average loss in energy upon collision is much higher when a neutron collides with atoms of low atomic weight, such as hydrogen. In soil, hydrogen is mainly present in water molecules, which effectively slows down the neutron compared to other elements present in the soil. This slowing down of the neutron increases the density of thermalised neutrons near the neutron probe. The density of the thermalised neutrons is proportional to the volumetric soil moisture. Some fraction of the slowed neutron returns to the probe, and the counter increments its value by 1. The actual volumetric moisture content is determined from the previously developed calibration curve that relates the volumetric moisture content with the count ratio (CR) [165], [166], as given below;

$$CR = \frac{C_{soil}}{C_{background}} \tag{A.6}$$

where C_{soil} is the actual count of the thermalised neutrons recorded in the counter and $C_{background}$ is the thermalised neutrons in the reference medium. CR is considered rather than the actual count of the neutrons received to enhance the experimental reproducibility. Challenges involved in operating neutron probes are: (i) the access tube should not be so thick that it itself contributes to the thermalisation process, (ii) the access tube must be made up of non-corrosive material; otherwise, it will start absorbing the neutrons, (iii) should not be any air void present between the tube and the soil matrix, and (iv) contains radioactive substances. Although the neutron probe provides much reliable soil moisture information at multi-depth, it fails to provide accurate moisture information at lower depths because a fraction of the neutrons escape from the soil surface into the air [167].

In contrast to the neutron probe, the gamma-ray probe measures the soil moisture by directly emitting the gamma-ray into the desired location along the soil column. It essentially consists of two separate systems: (1) a radiation system that includes a radioactive source and electronic parts to measure the intensity of the desired gamma-radiation energy levels; and (2) a transportation system for elevating and lowering the core of undisturbed soil in relation to the radioactive source and detector. Any substance through this radiation passes, including soil solids, soil-water, and the container housing the soil, absorbs some of it. The quantity of gamma radiation absorbed by the soil-water can be calculated by separately estimating the densities and thicknesses or widths of the soil system and container. The amount of radiation that passes through soil reduces as its water content increases. On the other hand, the amount of radiation traveling through a soil system increases as its water content drops [168]. Meanwhile, the use of the gamma-ray probe method is restricted to the laboratory, as it can scan a thin layer only, and the operation cost of the gamma-ray technique is relatively high. The advantage of the gamma-ray probe over the neutron probe is that it provides accurate measurement of soil moisture information for the upper layer of the soil surface, *i.e.,* a few centimeters below the air-soil interface.

C. SOIL-WATER DIELECTRIC TECHNIQUES: TIME DOMAIN AND FREQUENCY DOMAIN REFLECTOMETRY

Both neutron and gamma-ray probes were the dominating techniques for many decades until a group of Canadian geophysicists came up with the concept of utilising dielectric properties of soil to measure the moisture content [169]. Both TDR and FDR measure the soil-water mixture's dielectric constant to estimate the soil moisture content. As the dielectric constant, ϵ, of soil is 2, pure water is $\approx$80, and of the soil-water mixture is between $2 \sim 40$, it creates a gradient between pure water and soil with soil-water mixture ranging from very dry to very wet [29]. The behaviour of electromagnetic (EM) waves from frequencies ranging from 1 to 1000 MHz in the soil is used to measure this gradient in ϵ. It is then converted to volumetric moisture through the calibration equation.

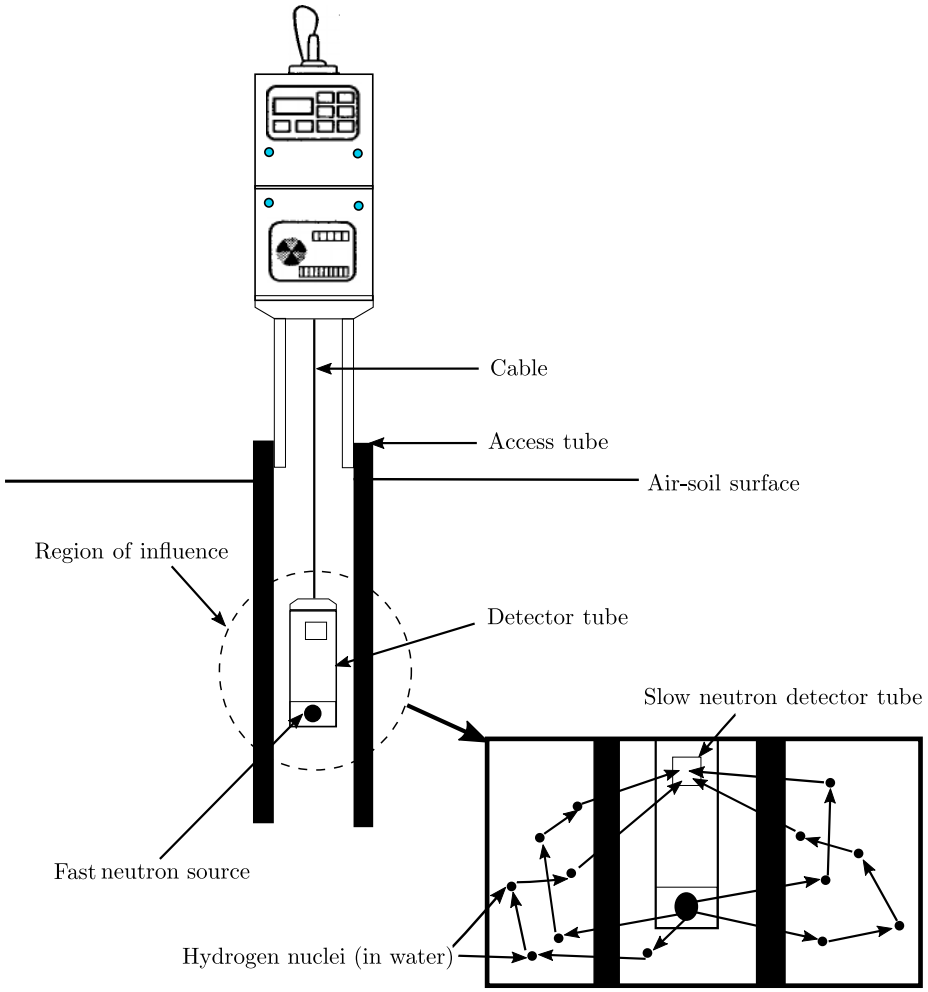

FIGURE 16. Schematic diagram of a neutron probe instrument.

TDR determines the bulk dielectric constant, ϵ_b, of the soil from travel time analysis from which the volumetric moisture content is calculated. The travel time, t, of the EM pulse or wave initiated along the wave-guide (formed by the parallel rods of length, L, with soil as the dielectric material in between) is calculated. The propagation velocity can be calculated, v, by $v = (2L/t)$ through the travel time analysis. As the EM pulse has to travel the rod twice (down and back), $2L$ length is considered. After calculating v, the ϵ_b is calculated by

$$\epsilon_b = \left(\frac{c}{v}\right)^2 = \left(\frac{ct}{2L}\right)^2 \tag{A.7}$$

where c is the speed of light (EM pulse) in vacuum (3×10^8 m/s). The travel time for the TDR-generated EM pulse (essentially a step signal) and its reflection is calculated based on the apparent length or the EM length of the TDR probe, which can be identified on the TDR output screen or the oscilloscope attached to it. The mark x_1 and x_2 in (Figure 17) represent the passing of the input step signal from epoxy to the probe and reflection from the end of the probe, respectively. The difference between the two marks, $x_2 - x_1$, gives the apparent length of the TDR probe. As the water content increases, so does the apparent length, which increases the soil's bulk dielectric constant. Both these parameters are related according to;

$$\epsilon_b = \left(\frac{x_2 - x_1}{V_p L}\right)^2 \tag{A.8}$$

where V_p represents the relative propagation velocity, it is user-specific and normally set to 0.99 [170]. The ϵ_b depends upon several factors such as the bulk density of the soil, soil porosity, measurement or operating frequency of the TDR, soil temperature, dipole moment (induced by water, air, or mineral), and water status (bound or free water). Various attempts to estimate volumetric moisture content from ϵ_b and consideration of the above-stated factor have resulted in the development of two models that establish a relationship between volumetric water content and ϵ_b. The first one is an empirical model developed by Topp et al. [171],

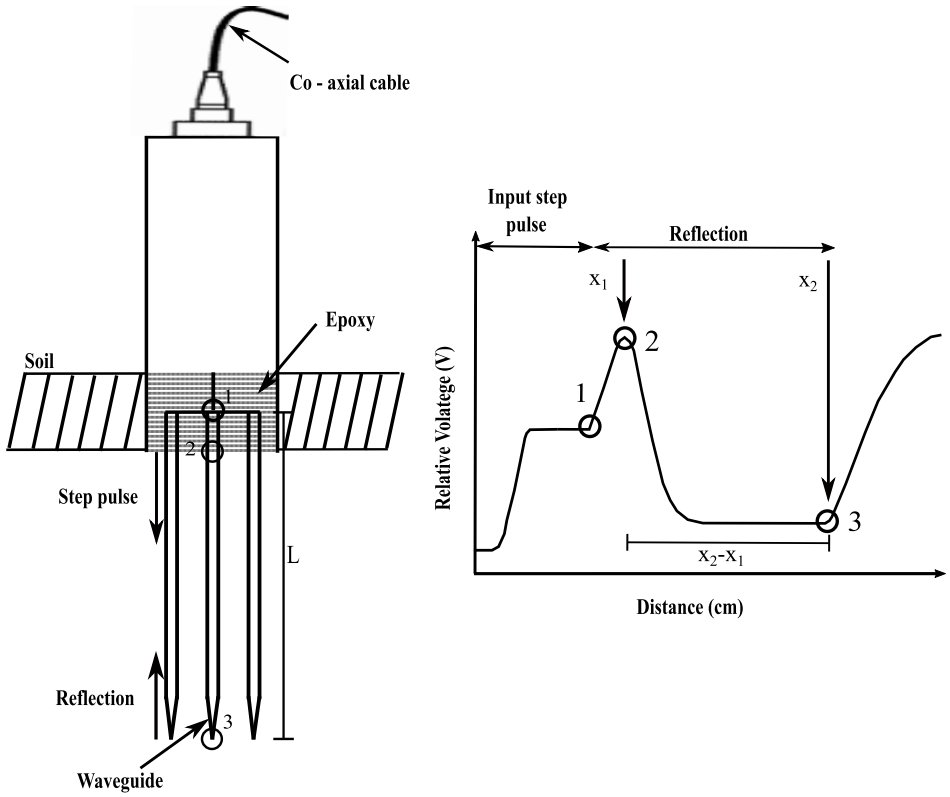

FIGURE 17. Schematic diagram of a Time-Domain Reflectometry (TDR) instrument.

while the second one was the dielectric mixing model proposed by Dobson et al. [172] in 1985. The TDR probes measure the soil moisture with high accuracy (within 1% or 2%), it does not contain radiation hazards, minimum calibration is required (soil specific calibration is not required), have minimal soil disturbance, and have high spatial and temporal resolution [170]. However, the TDR measurements can be affected by various factors, such as high saline and high conductive soils. High soil salinity and/or high conductive clay soil contributes to the attenuation of the reflected pulses that, in turn, overestimates the value of the dielectric constant and hence the soil moisture [173], [174]. Other disadvantages associated with TDR are a requirement of soil-specific calibration for soil having a high amount of bound water, relatively expensive, and small sensing volume capacity (around 1.2 inches around the wave-guide).

In contrast to TDR, the FDR probes are based on capacitance techniques. The probe consists of a pair of metallic plates/circular rings/rods placed in a plastic access tube. This arrangement forms a capacitor with soil as a dielectric. This capacitor is connected to an oscillator (operates at a frequency of 100 MHz) to form an electronically tuned circuit. The oscillator's operating frequency is controlled within a specified range to find the resonant frequency (peak amplitude), which is related to soil moisture [175]. Figure 18 illustrates a schematic diagram of the arrangement of multiple circular metallic ring-type sensors to measure soil moisture at different depths. FDR is a good alternative to the TDR in high-saline soils. It also has a better resolution than TDR and is relatively inexpensive due to the low-frequency circuits. A soil-specific calibration is required for FDR as it operates at a frequency lower than 100 MHz. At these frequencies, the bulk permittivity of the soil is more prone to change by the temperature, salinity, electrical conductivity, and clay content (Maxwell-Wagner effect) [176]. Commercially available capacitance sensors include $CS616 - L$ Water Content Reflectometer, ECH_2O probes (Decagon Devices, Inc.), and $CS620$ HydroSense® probe (Campbell Scientific), *HYDRA* probe (Stevens WMS, Inc.). (The manufacturer names are mentioned only for reference purposes).

Apart from TDR and FDR, Amplitude Domain Reflectometry (ADR), Phase Transmission (PT), and Time Domain Transmission (TDT) are also used for soil moisture estimation based on soil-water dielectrics [177]. The accuracy of all these instruments generally depends on the calibration, sensor type, material, and dry bulk density. The variance component analysis shows that the contribution of these factors is 42%, 29%, 18%, and 11%, respectively [178].

D. SOIL-WATER POTENTIAL TECHNIQUES: TENSIOMETER, RESISTANCE BLOCK, AND PSYCHROMETERS

Water content within different soils (*i.e.,* sand, silt, and clay) varies largely due to the huge variation in the particle surface

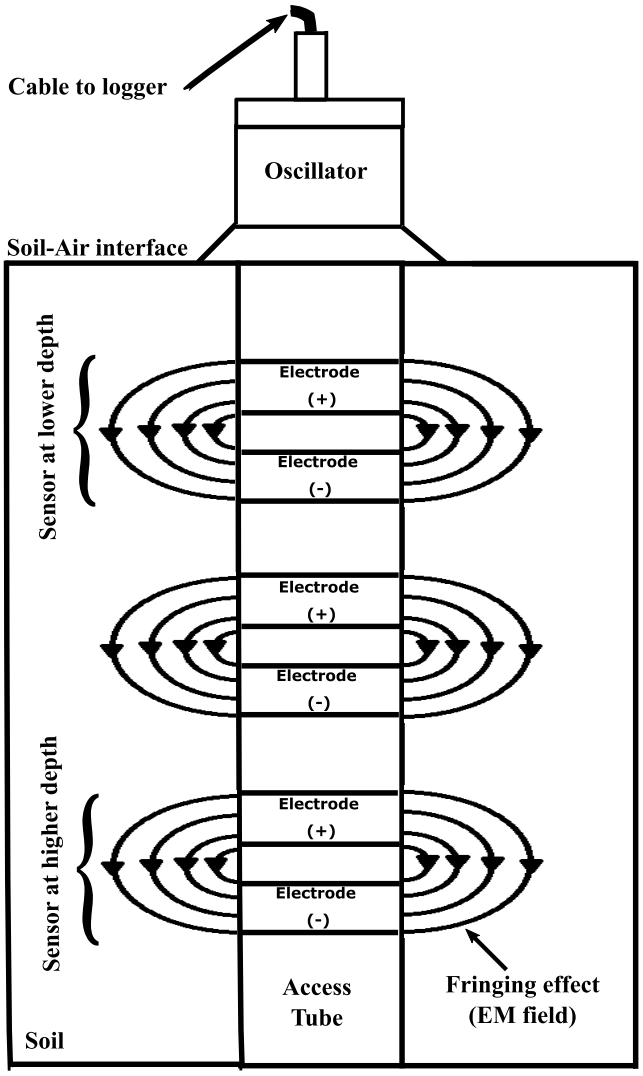

FIGURE 18. Schematic diagram of multiple Frequency Domain Reflectometry (FDR) sensors.

area. Water content is available at the Field Capacity (FC) and Permanent Wilting Point (PWP) are different for different soils. At FC, the water content in the sand is as low as 7 %, whereas in clay, it is around 40 %. Similarly, at PWP, the water content in sand ranges between 1 % to 2%, whereas in clay, it ranges between 25 % to 30 %. Therefore, the technique that best estimates the vegetation and crop water availability is the soil-water potential or tensiometric (also known as the energy status of water). It measures the relative amount of energy or work that is required to detach a unit of water from soil [179]. It is expressed in energy per unit mass [Jkg^{-1}], and it can be measured by several indirect techniques, such as tensiometers, resistance blocks, and psychrometers. All these methods measure how compact the soil holds the water but do not directly measure its water content. Also, none of these methods are capable of measuring the full range of possible soil-water potential values, *i.e.,* tensiometers perform well in the case of wet soil. In contrast, resistance blocks perform well in the case of dry soil.

Tensiometer measures the matric potential (a component of water potential) of the water. This instrument consists of a removable cap, a vacuum gauge at the top of the tube, and a porous ceramic cap at the bottom. The tube is filled with water, and it is inserted into the soil as illustrated in Figure 19. In the case of dry soil, the water flows out of the tensiometer, which results in the creation of a vacuum. The vacuum gauge measures the suction. The gauge reading is the direct measurement of the force required to remove water from the soil. Further, dryness in the soil results in higher vacuum readings. In contrast, the reverse process will occur when moisture is added to the soil. The moisture from the soil flows back into the tensiometer until the vacuum is reduced to its lowest possible value [180]. Nowadays, electronically governed pressure transducers are widely used instead of mechanical readers [181].

Apart from tensiometers, resistance blocks, and psychrometers are also used to measure the soil-water potential to estimate the soil moisture [182], [183]. Also, recently, a new technique [184] has been proposed for the measurement of soil suction and water content as deep as 7 m from the topsoil surface.

APPENDIX B RADAR BACKSCATTER MODELS

In this section, we review the most widely used radar backscatter models (Dubois model, Oh (1992, 1994, 2002, & 2004), Water Cloud Model (WCM), and Integral Equation Model) to indirectly predict the surface soil moisture.

A. DUBOIS MODEL

Dubois et al. [34] developed an empirical model based on the scatterometer and airborne datasets. It consists of two equations (*i.e.,* HH and VV) in terms of sensors and target parameters. The sensor parameters (*i.e.,* wavelength (λ) and incidence angle (θ)) are known for a specific satellite mission. The unknowns are the target parameters (*i.e.,* surface roughness (s) and soil permittivity (ϵ)). One can invert equations B.1 and B.2 simultaneously to get the two unknowns (s and ϵ). Once the soil permittivity is known, soil moisture can be estimated by using universal Topp's equation B.3.

$$\sigma^0_{HH} = 10^{-2.75}\left(\frac{cos^{1.5}\theta}{sin^5\theta}\right)10^{0.028\varepsilon tan\theta}(k.s.sin\theta)^{1.4}\lambda^{0.7} \tag{B.1}$$

$$\sigma^0_{VV} = 10^{-2.35}\left(\frac{cos^3\theta}{sin^3\theta}\right)10^{0.046\varepsilon tan\theta}(k.s.sin\theta)^{1.1}\lambda^{0.7} \tag{B.2}$$

$$m_v = -5.3\times10^{-2} + 2.92\times10^{-2}\epsilon - 5.5\times10^{-4}\epsilon^2 + 4.3\times10^{-6}\epsilon^3 \tag{B.3}$$

Dubois model performs well under the following validity conditions;

- It must be applied over bare and sparsely vegetated areas to obtain accurate results. It is applicable over

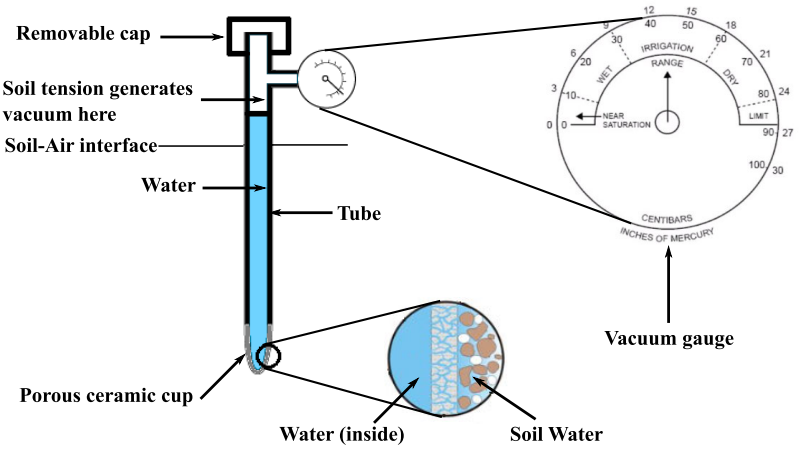

FIGURE 19. Schematic diagram of a tensiometer.

the area with NDVI < 0.4, known as the Dubois criterion. They have also established an equivalent relation corresponding to the Dubois criterion in terms of radar backscatter. They found that NDVI < 0.4 is equivalent to the cross-polarised ratio $\sigma^0_{HV}/\sigma^0_{VV}$ < -11dB (*i.e.,* $\sigma^0_{HV}/\sigma^0_{VV}$ < -11dB corresponds to NDVI < 0.4).
- It is valid only for the frequency range of 1.5 GHz to 11 GHz (*i.e.,* λ between 2.72 cm to 20 cm).
- The incidence angle of the SAR pulses θ, should be between 30^o to 65^o.
- It gives the best result for $k \cdot s \leq 2.5$ and $m_v \leq 0.35$.

B. OH MODELS

Oh et al. [31], [32], [33], [185] have proposed a series of empirical and semi-empirical models. Oh 1992 model relates the co-polarized (p=$\sigma^0_{HH}/\sigma^0_{VV}$) and cross-polarized (q=$\sigma^0_{HV}/\sigma^0_{VV}$) ratio with the sensor and target parameters. Like that of Dubois, we need to invert equations B.4 and B.5 simultaneously to estimate the surface roughness (or RMS height) and soil permittivity.

$$p = \frac{\sigma^o_{HH}}{\sigma^o_{VV}} = \left[1 - \left(\frac{\theta}{90^o}\right)^{1/3\Gamma_o} e^{-k.s}\right]^2 \tag{B.4}$$

$$q = \frac{\sigma^o_{HV}}{\sigma^o_{VV}} = 0.23\sqrt{\Gamma}_o(1 - e^{-k.s}) \tag{B.5}$$

where Γ_o is the Fresnel reflectivity of the surface at the nadir and is given by

$$\Gamma_o = \left|\frac{1 - \sqrt{\epsilon}}{1 + \sqrt{\epsilon}}\right|^2 \tag{B.6}$$

Oh 1992 model provides better results under the following conditions:
- This model is only applicable on the bare surface.
- It provides good agreement for $0.1 \leq ks \leq 6$, $2.5 \leq kl \leq 20$, and $0.09 \leq m_v \leq 0.31$.
- If the surface is rough, then this model may be used for $0^o \leq \theta \leq 70^o$, in contrast, if the surface is smooth, then this model may be used for $20^o \leq \theta \leq 70^o$

Later in 1994, Oh proposed a new expression for q to incorporate the effect of the incidence angle [185], and the corresponding model is known as Oh 1994 model.

$$q = \frac{\sigma^o_{HV}}{\sigma^o_{VV}} = 0.25\sqrt{\Gamma_o(0.1 + sin^{0.9}\theta)}(1 - e^{-[1.4-1.6\Gamma_o]k.s}) \tag{B.7}$$

Again in 2002, Oh modified the expression for p and q, and a new expression is proposed for σ^o_{HV} [32].

$$p = \frac{\sigma^o_{HH}}{\sigma^o_{VV}} = 1 - \left(\frac{\theta}{90^o}\right)^{0.35m_v^{-0.65}} e^{-0.4(k.s)^{1.4}} \tag{B.8}$$

$$q = \frac{\sigma^o_{HV}}{\sigma^o_{VV}} = 0.1\left(\frac{s}{l} + sin1.3\theta\right)^{1.2}(1 - e^{-0.9(k.s)^{0.8}}) \tag{B.9}$$

$$\sigma^o_{HV} = 0.11m_v^{0.7}cos^{2.2}\theta(1 - e^{-0.32(k.s)^{1.8}}) \tag{B.10}$$

Oh 2002 model has three equations (p, q, and σ^o_{HV}) with three unknowns namely m_v, s and l. First, the equations B.8 and B.9 need to be inverted to estimate m_v and s. Afterward, using the estimated s, we need to invert equation B.10 to calculate the correlation length, l.

Oh 2002 model gives the best results under the following condition:
- This model is only applicable on the bare surface.
- It provides good agreement for $0.13 \leq ks \leq 6.98$ and $0.04 \leq m_v \leq 0.291\ m^3/m^3$.
- The incidence angle, θ, should be between 10^o to 70^o.

Oh and Kay [186] and Baghdadi et al. [187] observed that the measurement of a correlation length, l, may not be correct. Also, the cross-polarisation ratio, q, in Oh 2002 model is insensitive to the roughness parameters, l. Motivated by this, Oh in 2004, proposed a new expression for q, which is

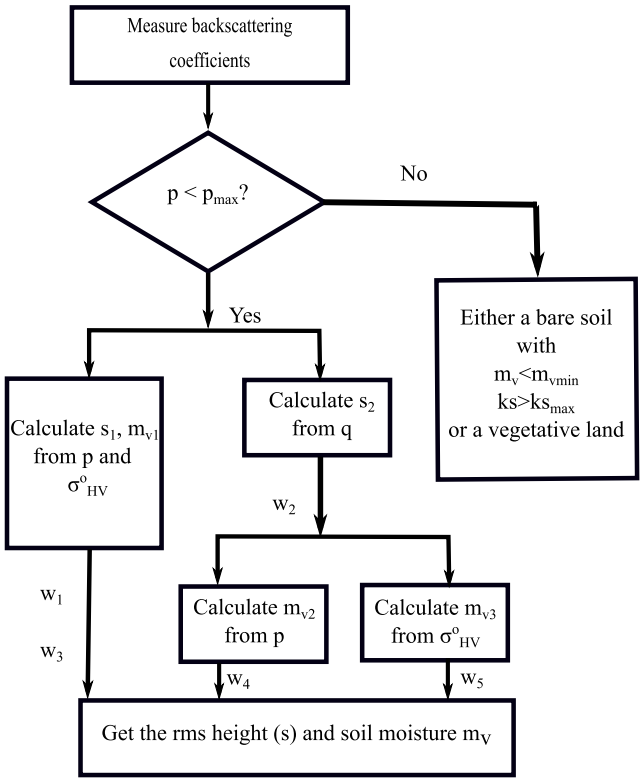

FIGURE 20. Computation of soil moisture and surface roughness from Oh 2004 model.

independent of the term l [33].

$$q = \frac{\sigma^o_{HV}}{\sigma^o_{VV}} = 0.095\left(0.13 + sin1.5\theta\right)^{1.4}(1 - e^{-1.3(k.s)^{0.9}}) \tag{B.11}$$

With the elimination of l, Oh 2004 model has three equations with two unknowns (m_v and s). Three values of m_v and two values of s are required to solve these equations. The final value of the soil moisture and surface roughness is calculated by the process explained in Figure 20. Here, p_{max} is calculated with maximum s (5.5 cm) and minimum m_v (0.01 cm^3/cm^3). The multiple estimates obtained are then averaged out by equations B.12 and B.13.

$$s = \frac{(w_1 s_1 + w_2 s_2)}{(w_1 + w_2)} \tag{B.12}$$

$$m_v = \frac{(w_3 m_{v1} + w_4 m_{v2})}{(w_5 + m_{v3})} \tag{B.13}$$

where w_1, w_2, w_3, w_4 and w_5 are weights. The value for w_1, w_2, w_3, w_4 and w_5 that gives the best inversion results are 1, 1/4, 1, 1 and 1, respectively.

This model gives the best results under the following conditions:

- This model is only applicable to the bare surface.
- It provides good agreement for $ks < 3.5$ and $m_v > [-6.286/ln(\theta/90)]^{-1.538}$

C. WATER CLOUD MODEL

A semi-empirical Water Cloud Model (WCM) was proposed by Attema and Ulaby [36]. It assumes the vegetation canopy as a cloud with water droplets embedded in it randomly. The model simulates the backscattering coefficient for the vegetation canopy as well as the underneath soil. WCM model has two assumptions:

- The shape and size of the vegetation layer are consistent and similar.
- It ignores the multiple scattering across vegetation and the Earth's surface.

Mathematically, the WCM can be expressed as;

$$\sigma^0_{pp} = \sigma^0_{veg} + L^2\sigma^0_{soil} \tag{B.14}$$

$$\sigma^0_{veg} = AV_1 cos\theta(1 - L^2) \tag{B.15}$$

$$L^2 = e^{(-2BV_2 sec\theta)} \tag{B.16}$$

where σ^0_{pp} is the total co-polarised backscattered coefficient, σ^0_{veg} is the backscatter contribution from the vegetation cover, σ^0_{soil} is the backscatter contribution from the soil surface, L^2 is the two way vegetation attenuation. A and B are the vegetation parameters where A represents the albedo of the vegetation and B represent the attenuation factor. V_1 and V_2 are the vegetation descriptors.

The radar backscattering contribution from the soil surface can be accurately extracted by subtracting the vegetation effect.

$$\sigma^0_{soil} = \frac{(\sigma^0_{pp} - \sigma^0_{veg})}{L^2} \tag{B.17}$$

The backscattering coefficient is a function of surface roughness and soil moisture. Among these two, the surface roughness remains unchanged for a short period; in that case, the change in the backscattering coefficient reflects the change in the soil moisture. The radar backscatter follows a linear relation with the soil moisture, which can be expressed as

$$\sigma^0_{soil} = C + D \cdot m_v \tag{B.18}$$

where C and D are bare soil parameters obtained from linear model fitting. The equation B.18 is inverted to calculate the soil moisture. The physical significance of the parameter D indicates the sensitivity of the radar signal to the soil moisture, and C represents the calibration constant.

D. INTEGRAL EQUATION MODEL

The Integral Equation Model (IEM) is the widely used theoretical backscattering model which is applicable for a validity range (Equations B.19 and B.20) that are commonly encountered for agriculture.

$$ks \leq 3 \tag{B.19}$$

$$\left(\frac{(kscos\theta)^2}{\sqrt{0.46kL}} exp\left(-\sqrt{0.92kL(1 - sin\theta)}\right)\right) < 0.25 \tag{B.20}$$

For bareland, the backscattering coefficient for co-polarisation (pp=HH or VV) is given by;

$$\sigma^0_{pp} = \frac{k}{2}|f_{pp}|^2 e^{-4k^2s^2cos^2\theta}\sum_{n=1}^{+\infty}\frac{(4k^2s^2cos^2\theta)^n}{n!}W^{(n)}(2ksin\theta,0) + \frac{k}{2}\Re\left(f^*_{pp}F_{pp}\right)e^{-3k^2s^2cos^2\theta}\sum_{n=1}^{+\infty}\frac{(4k^2s^2cos^2\theta)^n}{n!} \times W^{(n)}(2ksin\theta,0) + \frac{k}{8}|F_{pp}|^2 e^{-2k^2s^2cos^2\theta}\sum_{n=1}^{+\infty}\frac{(k^2s^2cos^2\theta)^n}{n!}W^{(n)}(2ksin\theta,0)$$

where $\Re$ is the real part of the complex number, f^*_{pp} is the conjugate of complex number f_{pp}. For cross-polarisation, the backscattering coefficient is given by

$$\sigma^0_{hv} = \frac{k}{16\pi}e^{-2k^2s^2cos^2\theta}\sum_{n=1}^{+\infty}\sum_{m=1}^{+\infty}\frac{(k^2s^2cos^2\theta)^{n+m}}{n!m!} \quad \text{(B.21)}$$

f_{hh} and f_{vv} is given by

$$f_{hh} = \frac{-2R_h}{cos\theta} \quad \text{(B.22)}$$

$$f_{vv} = \frac{2R_v}{cos\theta} \quad \text{(B.23)}$$

where R_h represents the Fresnel coefficient at horizontal polarisation

$$R_h = \frac{\mu_r cos\theta - \sqrt{\mu_r\epsilon_r - sin^2\theta}}{\mu_r cos\theta + \sqrt{\mu_r\epsilon_r - sin^2\theta}} \quad \text{(B.24)}$$

and R_v represents the Fresnel coefficient at vertical polarisation

$$R_v = \frac{\epsilon_r cos\theta - \sqrt{\mu_r\epsilon_r - sin^2\theta}}{\epsilon_r cos\theta + \sqrt{\mu_r\epsilon_r - sin^2\theta}} \quad \text{(B.25)}$$

F_{hh} and F_{vv} are given by

$$F_{hh} = \frac{2sin^2\theta}{cos\theta}\left[4\,R_h - \left(1-\frac{1}{\epsilon_r}\right)(1+R_h)^2\right] \quad \text{(B.26)}$$

$$F_{vv} = \frac{2sin^2\theta}{cos\theta}\left[\left(1-\frac{\epsilon_r cos^2\theta}{\mu_r\epsilon_r - sin^2\theta}\right)(1-R_v)^2 + \left(1-\frac{1}{\epsilon_r}\right)(1+R_v)^2\right] \quad \text{(B.27)}$$

$W^{(n)}$ is the Fourier transform of surface correlation function $\rho(x,y)$ given by

$$W^{(n)}(a,b) = \frac{1}{2\pi}\int\int \rho^n(x,y)e^{-i(ax+by)}dxdy \quad \text{(B.28)}$$

where $\rho(x,y)$ is exponential for low surface roughness value given by

$$\rho(x) = e^{-(\frac{x}{L})} \quad \text{(B.29)}$$

and $\rho(x,y)$ is Gaussian for high surface roughness value given by

$$\rho(x) = e^{-(\frac{x}{L})^2} \quad \text{(B.30)}$$

AUTHORS CONTRIBUTIONS

Abhilash Singh: conceptualization, methodology, software, validation, formal analysis, writing (original draft preparation), visualization, writing (review editing). Kumar Gaurav: investigation, software, resources, writing (original draft preparation), writing (review editing), visualization, supervision. Gaurav Kailash Sonkar: writing (original draft preparation), writing (review editing), visualization. Cheng-Chi Lee: investigation, writing (review editing), visualization.

COMPUTER CODE AVAILABILITY

We use publicly available software to execute the bibliometric analysis. The software can be downloaded from https://www.vosviewer.com/download. The codes for machine learning algorithms used in this study are available from the corresponding author upon reasonable request.

DATA AVAILABILITY

The datasets used/generated in this investigation are available from the corresponding author upon reasonable request.

CONFLICTS OF INTEREST (CoI)

The authors have no CoI to declare.

ACKNOWLEDGMENT

AS, KG, and GKS acknowledge the institutional support from IISER Bhopal. We acknowledge the editor and two anonymous reviewers for their constructive comments.

REFERENCES

[1] T. Zhao, J. Shi, L. Lv, H. Xu, D. Chen, Q. Cui, T. J. Jackson, G. Yan, L. Jia, and L. Chen, "Soil moisture experiment in the Luan river supporting new satellite mission opportunities," *Remote Sens. Environ.*, vol. 240, Apr. 2020, Art. no. 111680.
[2] J. M. Sabater, L. Jarlan, J.-C. Calvet, F. Bouyssel, and P. D. Rosnay, "From near-surface to root-zone soil moisture using different assimilation techniques," *J. Hydrometeorol.*, vol. 8, no. 2, pp. 194–206, Apr. 2007.
[3] G. W. Kite and A. Pietroniro, "Remote sensing applications in hydrological modelling," *Hydrolog. Sci. J.*, vol. 41, no. 4, pp. 563–591, Aug. 1996.
[4] T. J. Jackson, "III. Measuring surface soil moisture using passive microwave remote sensing," *Hydrol. Process.*, vol. 7, no. 2, pp. 139–152, 1993.
[5] D. Entekhabi, J. Nakamura, and E. Njoku, "Retrieval of soil moisture profile by combined remote sensing and modeling," Jet Propuls. Lab., California Inst. Technol. Pasadena, Pasadena, CA, USA, Tech. Rep. 0893, 1994.
[6] T. J. Jackson, M. E. Hawley, and P. E. O'Neill, "Preplanting soil moisture using passive microwave sensors," *J. Amer. Water Resour. Assoc.*, vol. 23, no. 1, pp. 11–19, Feb. 1987.
[7] M. E. Martin and J. D. Aber, "High spectral resolution remote sensing of forest canopy lignin, nitrogen, and ecosystem processes," *Ecolog. Appl.*, vol. 7, no. 2, pp. 431–443, May 1997.
[8] M. Sivapalan, K. Takeuchi, S. W. Franks, V. K. Gupta, H. Karambiri, V. Lakshmi, X. Liang, J. J. McDONNELL, E. M. Mendiondo, P. E. O'Connell, T. Oki, J. W. Pomeroy, D. Schertzer, S. Uhlenbrook, and E. Zehe, "IAHS decade on predictions in ungauged basins (PUB), 2003–2012: Shaping an exciting future for the hydrological sciences," *Hydrolog. Sci. J.*, vol. 48, no. 6, pp. 857–880, Dec. 2003.

[9] C. B. Field, J. T. Randerson, and C. M. Malmström, "Global net primary production: Combining ecology and remote sensing," *Remote Sens. Environ.*, vol. 51, no. 1, pp. 74–88, Jan. 1995.

[10] S. I. Seneviratne, "Investigating soil moisture–climate interactions in a changing climate: A review," *Earth-Sci. Rev.*, vol. 99, no. 3, pp. 125–161, May 2010.

[11] J. T. Kerr and M. Ostrovsky, "From space to species: Ecological applications for remote sensing," *Trends Ecol. Evol.*, vol. 18, no. 6, pp. 299–305, Jun. 2003.

[12] D. J. Mulla, "Twenty five years of remote sensing in precision agriculture: Key advances and remaining knowledge gaps," *Biosyst. Eng.*, vol. 114, no. 4, pp. 358–371, Apr. 2013.

[13] J. P. Walker, "Estimating soil moisture profile dynamics from near-surface soil moisture measurements and standard meteorological data," Ph.D. dissertation, Dept. Civil, Surveying Environ. Eng., Univ. Newcastle, Callaghan, NSW, Australia, 1999.

[14] H. L. McKim, J. E. Walsh, and D. Arion, "Review of techniques for measuring soil moisture in situ," Cold Regions Res. Engineering Lab, Hanover, NH, USA, Special Rep. 80-31, 1980.

[15] J. V. Stafford, "Remote, non-contact and in-situ measurement of soil moisture content: A review," *J. Agricult. Eng. Res.*, vol. 41, no. 3, pp. 151–172, Nov. 1988.

[16] F. S. Zazueta and J. Xin, "Soil moisture sensors," *Soil Sci.*, vol. 73, pp. 391–401, Apr. 1994.

[17] P. Ling, "A review of soil moisture sensors," *Assn. Flor. Prof. Bull.*, vol. 886, pp. 22–23, Jan. 2004.

[18] S. U. S. Lekshmi, D. N. Singh, and M. S. Baghini, "A critical review of soil moisture measurement," *Measurement*, vol. 54, pp. 92–105, Aug. 2014.

[19] M. Hardie, "Review of novel and emerging proximal soil moisture sensors for use in agriculture," *Sensors*, vol. 20, no. 23, p. 6934, Dec. 2020.

[20] E. Njoku and D. Entekhabi, "Passive microwave remote sensing of soil moisture," *J. Hydrol.*, vol. 184, nos. 1–2, pp. 101–129, Oct. 1996.

[21] B. P. Mohanty, M. H. Cosh, V. Lakshmi, and C. Montzka, "Soil moisture remote sensing: State-of-the-science," *Vadose Zone J.*, vol. 16, no. 1, pp. 1–9, 2017.

[22] E. Babaeian, M. Sadeghi, S. B. Jones, C. Montzka, H. Vereecken, and M. Tuller, "Ground, proximal, and satellite remote sensing of soil moisture," *Rev. Geophys.*, vol. 57, no. 2, pp. 530–616, 2019.

[23] A. Balenzano, "Sentinel-1 soil moisture at 1 km resolution: A validation study," *Remote Sens. Environ.*, vol. 263, Sep. 2021, Art. no. 112554.

[24] D. Baldwin, S. Manfreda, H. Lin, and E. A. H. Smithwick, "Estimating root zone soil moisture across the eastern United States with passive microwave satellite data and a simple hydrologic model," *Remote Sens.*, vol. 11, no. 17, p. 2013, Aug. 2019.

[25] S. O. and R. Orth, "Global soil moisture data derived through machine learning trained with in-situ measurements," *Sci. Data*, vol. 8, no. 1, pp. 1–14, Jul. 2021.

[26] A.-K. Ahlmer, M. Cavalli, K. Hansson, A. J. Koutsouris, S. Crema, and Z. Kalantari, "Soil moisture remote-sensing applications for identification of flood-prone areas along transport infrastructure," *Environ. Earth Sci.*, vol. 77, no. 14, pp. 1–17, Jul. 2018.

[27] Y. Li, S. Yan, N. Chen, and J. Gong, "Performance evaluation of a neural network model and two empirical models for estimating soil moisture based on Sentinel-1 SAR data," *Prog. Electromagn. Res. C*, vol. 105, pp. 85–99, 2020.

[28] E. Altese, O. Bolognani, M. Mancini, and P. A. Troch, "Retrieving soil moisture over bare soil from ERS 1 synthetic aperture radar data: Sensitivity analysis based on a theoretical surface scattering model and field data," *Water Resour. Res.*, vol. 32, no. 3, pp. 653–661, 1996.

[29] F. T. Ulaby, R. K. Moore, and A. K. Fung, "Microwave remote sensing: Active and passive. Volume 3-from theory to applications," Univ. Michigan, Ann Arbor, MI, USA, Tech. Rep. 19860041708, 1986.

[30] B. W. Barrett, E. Dwyer, and P. Whelan, "Soil moisture retrieval from active spaceborne microwave observations: An evaluation of current techniques," *Remote Sens.*, vol. 1, no. 3, pp. 210–242, 2009.

[31] Y. Oh, K. Sarabandi, and F. T. Ulaby, "An empirical model and an inversion technique for radar scattering from bare soil surfaces," *IEEE Trans. Geosci. Remote Sens.*, vol. 30, no. 2, pp. 370–381, Mar. 1992.

[32] Y. Oh, K. Sarabandi, and F. T. Ulaby, "Semi-empirical model of the ensemble-averaged differential Mueller matrix for microwave backscattering from bare soil surfaces," *IEEE Trans. Geosci. Remote Sens.*, vol. 40, no. 6, pp. 1348–1355, Jun. 2002.

[33] Y. Oh, "Quantitative retrieval of soil moisture content and surface roughness from multipolarized radar observations of bare soil surfaces," *IEEE Trans. Geosci. Remote Sens.*, vol. 42, no. 4, pp. 596–601, Mar. 2004.

[34] P. C. Dubois, J. J. van Zyl, and T. Engman, "Measuring soil moisture with imaging radars," *IEEE Trans. Geosci. Remote Sens.*, vol. 33, no. 4, pp. 915–926, Jul. 1995.

[35] A. K. Fung, Z. Li, and K. S. Chen, "Backscattering from a randomly rough dielectric surface," *IEEE Trans. Geosci. Remote Sens.*, vol. 30, no. 2, pp. 356–369, Mar. 1992.

[36] E. P. W. Attema and F. T. Ulaby, "Vegetation modeled as a water cloud," *Radio Sci.*, vol. 13, no. 2, pp. 357–364, Mar./Apr. 1978.

[37] M. R. Sahebi and J. Angles, "An inversion method based on multi-angular approaches for estimating bare soil surface parameters from RADARSAT-1," *Hydrol. Earth Syst. Sci.*, vol. 14, no. 11, pp. 2355–2366, Nov. 2010.

[38] S. K. Kweon and Y. Oh, "A modified water-cloud model with leaf angle parameters for microwave backscattering from agricultural fields," *IEEE Trans. Geosci. Remote Sens.*, vol. 53, no. 5, pp. 2802–2809, May 2015.

[39] T. Svoray and M. Shoshany, "SAR-based estimation of areal above-ground biomass (AAB) of herbaceous vegetation in the semi-arid zone: A modification of the water-cloud model," *Int. J. Remote Sens.*, vol. 23, no. 19, pp. 4089–4100, Jan. 2002.

[40] V. P. Yadav, R. Prasad, R. Bala, and A. K. Vishwakarma, "An improved inversion algorithm for spatio–temporal retrieval of soil moisture through modified water cloud model using C-band Sentinel-1A SAR data," *Comput. Electron. Agricult.*, vol. 173, Jun. 2020, Art. no. 105447.

[41] A. Singh, K. Gaurav, G. K. Meena, and S. Kumar, "Estimation of soil moisture applying modified Dubois model to Sentinel-1; a regional study from central India," *Remote Sens.*, vol. 12, no. 14, p. 2266, Jul. 2020.

[42] C. Dirksen, *Soil Physics Measurements*. Stuttgart, Germany: Schweizerbart Science Publishers, Jan. 1998.

[43] W. A. Dorigo, "The international soil moisture network: A data hosting facility for global in situ soil moisture measurements," *Hydrol. Earth Syst. Sci.*, vol. 15, no. 5, pp. 1675–1698, 2011.

[44] W. Dorigo, P. Oevelen, W. Wagner, M. Drusch, S. Mecklenburg, A. Robock, and T. Jackson, "A new international network for in situ soil moisture data," *Eos, Trans. Amer. Geophys. Union*, vol. 92, no. 17, pp. 141–142, Apr. 2011.

[45] A. Gruber, W. A. Dorigo, S. Zwieback, A. Xaver, and W. Wagner, "Characterizing coarse-scale representativeness of in situ soil moisture measurements from the international soil moisture network," *Vadose Zone J.*, vol. 12, no. 2, May 2013, Art. no. vzj2012.0170.

[46] W. Dorigo, "The international soil moisture network: Serving Earth system science for over a decade," *Hydrol. Earth Syst. Sci.*, vol. 25, no. 11, pp. 5749–5804, 2021.

[47] I. Himmelbauer, L. Zappa, A. Xaver, and W. Dorigo, "The international soil moisture network and its benefit for soil moisture product validation," in *Proc. EGU Gen. Assem. Conf. Abstr.*, vol. 20, 2018, p. 15923.

[48] S. G. Reynolds, "The gravimetric method of soil moisture determination—Part I a study of equipment, and methodological problems," *J. Hydrol.*, vol. 11, no. 3, pp. 258–273, Sep. 1970.

[49] V. Francesca, F. Osvaldo, P. Stefano, and R. P. Paola, "Soil moisture measurements: Comparison of instrumentation performances," *J. Irrigation Drainage Eng.*, vol. 136, no. 2, pp. 81–89, Feb. 2010.

[50] J. D. Shinn, D. A. Timian, R. M. Morey, G. Mitchell, C. L. Antle, and R. Hull, "Development of a CPT deployed probe forin situ measurement of volumetric soil moisture content and electrical resistivity," *Field Anal. Chem. Technol.*, vol. 2, no. 2, pp. 103–109, 1998.

[51] D. A. Robinson, S. B. Jones, J. M. Wraith, D. Or, and S. P. Friedman, "A review of advances in dielectric and electrical conductivity measurement in soils using time domain reflectometry," *Vadose Zone J.*, vol. 2, no. 4, pp. 444–475, 2003.

[52] S. R. Evett, R. C. Schwartz, J. A. Tolk, and T. A. Howell, "Soil profile water content determination: Spatiotemporal variability of electromagnetic and neutron probe sensors in access tubes," *Vadose Zone J.*, vol. 8, no. 4, pp. 926–941, Nov. 2009.

[53] O. Bacchi, K. Reichart, and M. Calvache, "Neutron and gamma probes: Their use in agronomy," Int. Atomic Energy Agency, Vienna, Austria, Tech. Rep. IAEA-TCS–16, 2002.

[54] T. S. Freitas, A. S. Guimarães, S. Roels, V. P. de Freitas, and A. Cataldo, "Is the time-domain reflectometry (TDR) technique suitable for moisture content measurement in low-porosity building materials?" *Sustainability*, vol. 12, no. 19, p. 7855, Sep. 2020.

[55] E. R. Ojo, P. R. Bullock, J. L'Heureux, J. Powers, H. McNairn, and A. Pacheco, "Calibration and evaluation of a frequency domain reflectometry sensor for real-time soil moisture monitoring," *Vadose Zone J.*, vol. 14, no. 3, Mar. 2015, Art. no. vzj2014.08.0114.

[56] E. Veldkamp and J. J. O'Brien, "Calibration of a frequency domain reflectometry sensor for humid tropical soils of volcanic origin," *Soil Sci. Soc. Amer. J.*, vol. 64, no. 5, pp. 1549–1553, Sep. 2000.

[57] P. Dobriyal, A. Qureshi, R. Badola, and S. A. Hussain, "A review of the methods available for estimating soil moisture and its implications for water resource management," *J. Hydrol.*, vols. 458–459, pp. 110–117, Aug. 2012.

[58] I. White and S. Zegelin, "Electric and dielectric methods for monitoring soil-water content," in *Handbook of Vadose Zone Characterization & Monitoring*. Boca Raton, FL, USA: CRC Press, 2018, pp. 343–385.

[59] R. Montgomery and R. McDowall, *Fundamentals of HVAC Control Systems*. Amsterdam, The Netherlands: Elsevier, 2008.

[60] N. J. P. Anne, A. H. Abd-Elrahman, D. B. Lewis, and N. A. Hewitt, "Modeling soil parameters using hyperspectral image reflectance in subtropical coastal wetlands," *Int. J. Appl. Earth Observ. Geoinf.*, vol. 33, pp. 47–56, Dec. 2014.

[61] R. Filion, M. Bernier, C. Paniconi, K. Chokmani, M. Melis, A. Soddu, M. Talazac, and F.-X. Lafortune, "Remote sensing for mapping soil moisture and drainage potential in semi-arid regions: Applications to the Campidano plain of Sardinia, Italy," *Sci. Total Environ.*, vol. 543, pp. 862–876, Feb. 2016.

[62] D. Zhang and G. Zhou, "Estimation of soil moisture from optical and thermal remote sensing: A review," *Sensors*, vol. 16, no. 8, p. 1308, Aug. 2016.

[63] S. A. Bowers and S. J. Smith, "Spectrophotometric determination of soil water content," *Soil Sci. Soc. Amer. J.*, vol. 36, no. 6, pp. 978–980, Nov. 1972.

[64] W. T. Liu and A. A. Ferreira, "Monitoring crop production regions in the Sao Paulo state of Brazil using normalized difference vegetation index," Environ. Res. Inst. Michigan, Ann Arbor, MI, USA, Tech. Rep., 1991, pp. 447–455, vol. 2. [Online]. Available: https://repositorio.usp.br/item/000832721

[65] Y. Han, Y. Wang, and Y. Zhao, "Estimating soil moisture conditions of the greater Changbai Mountains by land surface temperature and NDVI," *IEEE Trans. Geosci. Remote Sens.*, vol. 48, no. 6, pp. 2509–2515, Jun. 2010.

[66] J. C. Price, "Using spatial context in satellite data to infer regional scale evapotranspiration," *IEEE Trans. Geosci. Remote Sens.*, vol. 28, no. 5, pp. 940–948, Sep. 1990.

[67] D. Zhang, R. Tang, B.-H. Tang, H. Wu, and Z.-L. Li, "A simple method for soil moisture determination from LST–VI feature space using nonlinear interpolation based on thermal infrared remotely sensed data," *IEEE J. Sel. Topics Appl. Earth Observ. Remote Sens.*, vol. 8, no. 2, pp. 638–648, Feb. 2015.

[68] R. Jackson, "Detection of water stress in wheat by measurement of reflected solar and emitted thermal IR radiation," in *Proc. Signatures Spectrales d'objets en Teledetection*, 1981, pp. 399–406.

[69] X. Song, P. Leng, X. Li, X. Li, and J. Ma, "Retrieval of daily evolution of soil moisture from satellite-derived Land Surface Temperature and net surface shortwave radiation," *Int. J. Remote Sens.*, vol. 34, nos. 9–10, pp. 3289–3298, May 2013.

[70] E. T. Engman, "Applications of microwave remote sensing of soil moisture for water resources and agriculture," *Remote Sens. Environ.*, vol. 35, nos. 2–3, pp. 213–226, Feb. 1991.

[71] D. Luo, X. Wen, and J. Xu, "All-sky soil moisture estimation over agriculture areas from the full polarimetric SAR GF-3 data," *Sustainability*, vol. 14, no. 17, Aug. 2022, Art. no. 10866.

[72] M. Xing, L. Chen, J. Wang, J. Shang, and X. Huang, "Soil moisture retrieval using SAR backscattering ratio method during the crop growing season," *Remote Sens.*, vol. 14, no. 13, p. 3210, Jul. 2022.

[73] V. Shashikant, A. R. Mohamed Shariff, A. Wayayok, M. R. Kamal, Y. P. Lee, and W. Takeuchi, "Vegetation effects on soil moisture retrieval from water cloud model using PALSAR-2 for oil palm trees," *Remote Sens.*, vol. 13, no. 20, p. 4023, Oct. 2021.

[74] M. Yang, H. Wang, C. Tong, L. Zhu, X. Deng, J. Deng, and K. Wang, "Soil moisture retrievals using multi-temporal Sentinel-1 data over Nagqu region of Tibetan Plateau," *Remote Sens.*, vol. 13, no. 10, p. 1913, May 2021.

[75] C. Ma, X. Li, and M. F. McCabe, "Retrieval of high-resolution soil moisture through combination of Sentinel-1 and Sentinel-2 data," *Remote Sens.*, vol. 12, no. 14, p. 2303, Jul. 2020.

[76] Y. Liu, J. Qian, and H. Yue, "Combined Sentinel-1A with Sentinel-2A to estimate soil moisture in farmland," *IEEE J. Sel. Topics Appl. Earth Observ. Remote Sens.*, vol. 14, pp. 1292–1310, 2021.

[77] J. Ezzahar, N. Ouaadi, M. Zribi, J. Elfarkh, G. Aouade, S. Khabba, S. Er-Raki, A. Chehbouni, and L. Jarlan, "Evaluation of backscattering models and support vector machine for the retrieval of bare soil moisture from Sentinel-1 data," *Remote Sens.*, vol. 12, no. 1, p. 72, Dec. 2019.

[78] M. Zribi, S. Muddu, S. Bousbih, A. Al Bitar, S. K. Tomer, N. Baghdadi, and S. Bandyopadhyay, "Analysis of L-band SAR data for soil moisture estimations over agricultural areas in the tropics," *Remote Sens.*, vol. 11, no. 9, p. 1122, May 2019.

[79] J. Li and S. Wang, "Using SAR-derived vegetation descriptors in a water cloud model to improve soil moisture retrieval," *Remote Sens.*, vol. 10, no. 9, p. 1370, Aug. 2018.

[80] K. Y. Kondratyev, V. Melentyev, Y. I. Rabinovich, and E. Shulgina, "Passive microwave remote sensing of soil moisture," in *Proc. ERIM 11th Intern. Symp. Remote Sens. Environ.*, vol. 2, 1977, pp. 1–33.

[81] A. E. Basharinov, M. S. Krylova, A. I. Maslov, and A. M. Shutko, "Remote sensing of subsurface soil moisture by means of microwave radiometers," *Water Resour.*, vol. 5, pp. 538–542, 1979.

[82] T. J. Jackson, "Survey of applications of passive microwave remote sensing for soil moisture in the USSR," *Eos, Trans. Amer. Geophys. Union*, vol. 63, no. 19, pp. 497–499, 1982.

[83] T. J. Jackson and T. J. Schmugge, "Passive microwave remote sensing of soil moisture," *Adv. Hydrosci.*, vol. 14, pp. 123–159, Oct. 1986.

[84] G. Gutman and L. Rukhovetz, "Towards satellite-derived global estimation of monthly evapotranspiration over land surfaces," *Adv. Space Res.*, vol. 18, no. 7, pp. 67–71, Jan. 1996.

[85] Y. Du, F. T. Ulaby, and M. C. Dobson, "Sensitivity to soil moisture by active and passive microwave sensors," *IEEE Trans. Geosci. Remote Sens.*, vol. 38, no. 1, pp. 105–114, Jan. 2000.

[86] S. Paloscia, G. Macelloni, E. Santi, and T. Koike, "A multifrequency algorithm for the retrieval of soil moisture on a large scale using microwave data from SMMR and SSM/I satellites," *IEEE Trans. Geosci. Remote Sens.*, vol. 39, no. 8, pp. 1655–1661, Aug. 2001.

[87] E. G. Njoku, T. J. Jackson, V. Lakshmi, T. K. Chan, and S. V. Nghiem, "Soil moisture retrieval from AMSR-E," *IEEE Trans. Geosci. Remote Sens.*, vol. 41, no. 2, pp. 215–229, Feb. 2003.

[88] R. Bindlish, T. Jackson, M. Cosh, T. Zhao, and P. O'Neill, "Global soil moisture from the aquarius/SAC-D satellite: Description and initial assessment," *IEEE Geosci. Remote Sens. Lett.*, vol. 12, no. 5, pp. 923–927, May 2015.

[89] R. Akbar, N. Das, D. Entekhabi, and M. Moghaddam, "Active and passive microwave remote sensing synergy for soil moisture estimation," in *Satellite Soil Moisture Retrieval*. Amsterdam, The Netherlands: Elsevier, 2016, pp. 187–207.

[90] D. Li, T. Zhao, J. Shi, R. Bindlish, T. J. Jackson, B. Peng, M. An, and B. Han, "First evaluation of aquarius soil moisture products using in situ observations and GLDAS model simulations," *IEEE J. Sel. Topics Appl. Earth Observ. Remote Sens.*, vol. 8, no. 12, pp. 5511–5525, Dec. 2015.

[91] M. S. Burgin, "A comparative study of the SMAP passive soil moisture product with existing satellite-based soil moisture products," *IEEE Trans. Geosci. Remote Sens.*, vol. 55, no. 5, pp. 2959–2971, May 2017.

[92] Z. Wang, T. Che, T. Zhao, L. Dai, X. Li, and J.-P. Wigneron, "Evaluation of SMAP, SMOS, and AMSR2 soil moisture products based on distributed ground observation network in cold and arid regions of China," *IEEE J. Sel. Topics Appl. Earth Observ. Remote Sens.*, vol. 14, pp. 8955–8970, 2021.

[93] R. D. Magagi and Y. H. Kerr, "Retrieval of soil moisture and vegetation characteristics by use of ERS-1 wind scatterometer over arid and semi-arid areas," *J. Hydrol.*, vols. 188–189, pp. 361–384, Feb. 1997.

[94] J. T. Pulliainen, T. Manninen, and M. T. Hallikainen, "Application of ERS-1 wind scatterometer data to soil frost and soil moisture monitoring in boreal forest zone," *IEEE Trans. Geosci. Remote Sens.*, vol. 36, no. 3, pp. 849–863, May 1998.

[95] W. Wagner, G. Lemoine, and H. Rott, "A method for estimating soil moisture from ERS scatterometer and soil data," *Remote Sens. Environ.*, vol. 70, no. 2, pp. 191–207, Nov. 1999.

[96] A. Singh, M. N. Naik, and K. Gaurav, "Drainage congestion due to road network on the Kosi alluvial fan, Himalayan foreland," *Int. J. Appl. Earth Observ. Geoinf.*, vol. 112, Aug. 2022, Art. no. 102892.

[97] E. Santi, S. Paloscia, S. Pettinato, and G. Fontanelli, "Application of artificial neural networks for the soil moisture retrieval from active and passive microwave spaceborne sensors," *Int. J. Appl. Earth Observ. Geoinf.*, vol. 48, pp. 61–73, Jun. 2016.

[98] N. J. van Eck and L. Waltman, "Software survey: VOSviewer, a computer program for bibliometric mapping," *Scientometrics*, vol. 84, no. 2, pp. 523–538, 2010.

[99] S. H. H. Shah, S. Lei, M. Ali, D. Doronin, and S. T. Hussain, "Prosumption: Bibliometric analysis using HistCite and VOSviewer," *Kybernetes*, vol. 49, no. 3, pp. 1020–1045, 2020.

[100] J. A. Moral-Muñoz, E. Herrera-Viedma, A. Santisteban-Espejo, and M. J. Cobo, "Software tools for conducting bibliometric analysis in science: An up-to-date review," *El Profesional de la Información*, vol. 29, no. 1, pp. 1–20, Jan. 2020.

[101] N. Donthu, S. Kumar, D. Mukherjee, N. Pandey, and W. M. Lim, "How to conduct a bibliometric analysis: An overview and guidelines," *J. Bus. Res.*, vol. 133, pp. 285–296, Sep. 2021.

[102] N. J. Van Eck and L. Waltman, "Vosviewer manual," *Leiden, Univeristeit Leiden*, vol. 1, no. 1, pp. 1–53, 2013.

[103] L. Waltman, N. J. van Eck, and E. C. M. Noyons, "A unified approach to mapping and clustering of bibliometric networks," *J. Informetrics*, vol. 4, no. 4, pp. 629–635, Oct. 2010.

[104] J. L. C. Camargo and V. Kapos, "Complex edge effects on soil moisture and microclimate in central Amazonian forest," *J. Tropical Ecol.*, vol. 11, no. 2, pp. 205–221, May 1995.

[105] H. Li, A. Robock, S. Liu, X. Mo, and P. Viterbo, "Evaluation of reanalysis soil moisture simulations using updated Chinese soil moisture observations," *J. Hydrometeorol.*, vol. 6, no. 2, pp. 180–193, Apr. 2005.

[106] L. Brocca, R. Morbidelli, F. Melone, and T. Moramarco, "Soil moisture spatial variability in experimental areas of central Italy," *J. Hydrol.*, vol. 333, nos. 2–4, pp. 356–373, Feb. 2007.

[107] T. J. Kelleners, D. A. Robinson, P. J. Shouse, J. E. Ayars, and T. H. Skaggs, "Frequency dependence of the complex permittivity and its impact on dielectric sensor calibration in soils," *Soil Sci. Soc. Amer. J.*, vol. 69, no. 1, pp. 67–76, 2005.

[108] H. R. Bogena, J. A. Huisman, A. Güntner, C. Hübner, J. Kusche, F. Jonard, S. Vey, and H. Vereecken, "Emerging methods for noninvasive sensing of soil moisture dynamics from field to catchment scale: A review," *WIREs Water*, vol. 2, no. 6, pp. 635–647, Nov. 2015.

[109] L. Breiman, "Random forests," *Mach. Learn.*, vol. 45, no. 1, pp. 5–32, 2001.

[110] G. Biau, "Analysis of a random forests model," *J. Mach. Learn. Res.*, vol. 13, pp. 1063–1095, Apr. 2012.

[111] S. Ahmad, A. Kalra, and H. Stephen, "Estimating soil moisture using remote sensing data: A machine learning approach," *Adv. water Resour.*, vol. 33, no. 1, pp. 69–80, 2010.

[112] G. Ayehu, T. Tadesse, B. Gessesse, Y. Yigrem, and A. M. Melesse, "Combined use of Sentinel-1 SAR and landsat sensors products for residual soil moisture retrieval over agricultural fields in the Upper Blue Nile basin, Ethiopia," *Sensors*, vol. 20, no. 11, p. 3282, Jun. 2020.

[113] M. Leshno, V. Y. Lin, A. Pinkus, and S. Schocken, "Multilayer feedforward networks with a nonpolynomial activation function can approximate any function," *Neural Netw.*, vol. 6, no. 6, pp. 861–867, 1993.

[114] P. Ferreira, P. Ribeiro, A. Antunes, and F. M. Dias, "A high bit resolution FPGA implementation of a FNN with a new algorithm for the activation function," *Neurocomputing*, vol. 71, nos. 1–3, pp. 71–77, Dec. 2007.

[115] J. Feng and S. Lu, "Performance analysis of various activation functions in artificial neural networks," *J. Phys., Conf. Ser.*, vol. 1237, no. 2, Jun. 2019, Art. no. 022030.

[116] P. Vlachas, "Backpropagation algorithms and reservoir computing in recurrent neural networks for the forecasting of complex spatiotemporal dynamics," *Neural Netw.*, vol. 126, pp. 191–217, Jun. 2020.

[117] M. H. Sazli, "A brief review of feed-forward neural networks," Commun. Fac. Sci. Univ. Ankara Ser. A2–A3 Phys. Sci. Eng., Turkey, Tech. Rep., 2006, vol. 50, no. 1, doi: 10.1501/commua1-2_0000000026.

[118] V. K. Ojha, A. Abraham, and V. Snášel, "Metaheuristic design of feedforward neural networks: A review of two decades of research," *Eng. Appl. Artif. Intell.*, vol. 60, pp. 97–116, Apr. 2017.

[119] V. Vapnik, *The Nature of Statistical Learning Theory*. Cham, Switzerland: Springer, 1999.

[120] H. Drucker, C. J. Burges, L. Kaufman, A. J. Smola, and V. Vapnik, "Support vector regression machines," in *Proc. Neural Inf. Process. Syst.*, vol. 9, 1997, pp. 155–161.

[121] G. Mountrakis, J. Im, and C. Ogole, "Support vector machines in remote sensing: A review," *ISPRS J. Photogramm. Remote Sens.*, vol. 66, no. 3, pp. 247–259, May 2011.

[122] P.-S. Yu, S.-T. Chen, and I.-F. Chang, "Support vector regression for real-time flood stage forecasting," *J. Hydrol.*, vol. 328, nos. 3–4, pp. 704–716, Sep. 2006.

[123] X. Xiao, T. Zhang, X. Zhong, W. Shao, and X. Li, "Support vector regression snow-depth retrieval algorithm using passive microwave remote sensing data," *Remote Sens. Environ.*, vol. 210, pp. 48–64, Jun. 2018.

[124] S. Kuter, "Completing the machine learning saga in fractional snow cover estimation from MODIS Terra reflectance data: Random forests versus support vector regression," *Remote Sens. Environ.*, vol. 255, Mar. 2021, Art. no. 112294.

[125] J. Ge, B. P. Meng, T. Liang, Q. Feng, J. Gao, S. Yang, X. Huang, and H. Xie, "Modeling Alpine grassland cover based on MODIS data and support vector machine regression in the headwater region of the Huanghe River, China," *Remote Sens. Environ.*, vol. 218, pp. 162–173, Dec. 2018.

[126] X. Xie, W. Liu, and B. Tang, "Spacebased estimation of moisture transport in marine atmosphere using support vector regression," *Remote Sens. Environ.*, vol. 112, no. 4, pp. 1846–1855, Apr. 2008.

[127] A. Okujeni, S. van der Linden, L. Tits, B. Somers, and P. Hostert, "Support vector regression and synthetically mixed training data for quantifying urban land cover," *Remote Sens. Environ.*, vol. 137, pp. 184–197, Oct. 2013.

[128] H. Su, X. Wu, X.-H. Yan, and A. Kidwell, "Estimation of subsurface temperature anomaly in the Indian Ocean during recent global surface warming hiatus from satellite measurements: A support vector machine approach," *Remote Sens. Environ.*, vol. 160, pp. 63–71, Apr. 2015.

[129] A. Malik, Y. Tikhamarine, D. Souag-Gamane, P. Rai, S. S. Sammen, and O. Kisi, "Support vector regression integrated with novel meta-heuristic algorithms for meteorological drought prediction," *Meteorol. Atmos. Phys.*, vol. 133, pp. 891–909, Jun. 2021.

[130] M. Awad and R. Khanna, "Support vector regression," in *Efficient Learning Machines*. Cham, Switzerland: Springer, 2015, pp. 67–80.

[131] A. Singh, V. Kotiyal, S. Sharma, J. Nagar, and C.-C. Lee, "A machine learning approach to predict the average localization error with applications to wireless sensor networks," *IEEE Access*, vol. 8, pp. 208253–208263, 2020.

[132] A. Singh, K. Gaurav, A. K. Rai, and Z. Beg, "Machine learning to estimate surface roughness from satellite images," *Remote Sens.*, vol. 13, no. 19, p. 3794, Sep. 2021.

[133] A. Singh and K. Gaurav, "Deep learning and data fusion to estimate surface soil moisture from multi-sensor satellite images," *Sci. Rep.*, vol. 13, no. 1, pp. 1–21, 2023.

[134] E. Babaeian, S. Paheding, N. Siddique, V. K. Devabhaktuni, and M. Tuller, "Estimation of root zone soil moisture from ground and remotely sensed soil information with multisensor data fusion and automated machine learning," *Remote Sens. Environ.*, vol. 260, Jul. 2021, Art. no. 112434.

[135] S. K. Chaudhary, P. K. Srivastava, D. K. Gupta, P. Kumar, R. Prasad, D. K. Pandey, A. K. Das, and M. Gupta, "Machine learning algorithms for soil moisture estimation using Sentinel-1: Model development and implementation," *Adv. Space Res.*, vol. 69, no. 4, pp. 1799–1812, Feb. 2022.

[136] Y. Cui, X. Chen, W. Xiong, L. He, F. Lv, W. Fan, Z. Luo, and Y. Hong, "A soil moisture spatial and temporal resolution improving algorithm based on multi-source remote sensing data and GRNN model," *Remote Sens.*, vol. 12, no. 3, p. 455, Feb. 2020.

[137] H. Adab, R. Morbidelli, C. Saltalippi, M. Moradian, and G. A. F. Ghalhari, "Machine learning to estimate surface soil moisture from remote sensing data," *Water*, vol. 12, no. 11, p. 3223, Nov. 2020.

[138] V. Senyurek, F. Lei, D. Boyd, M. Kurum, A. C. Gurbuz, and R. Moorhead, "Machine learning-based CYGNSS soil moisture estimates over ISMN sites in CONUS," *Remote Sens.*, vol. 12, no. 7, p. 1168, Apr. 2020.

[139] S. Araya, A. Fryjoff-Hung, A. Anderson, J. Viers, and T. Ghezzehei, "Advances in soil moisture retrieval from multispectral remote sensing using unmanned aircraft systems and machine learning techniques," *Hydrol. Earth Syst. Sci. Discuss*, vol. 2020, pp. 1–33, Aug. 2020.

[140] E. Santi, M. Dabboor, S. Pettinato, and S. Paloscia, "Combining machine learning and compact polarimetry for estimating soil moisture from C-band SAR data," *Remote Sens.*, vol. 11, no. 20, p. 2451, Oct. 2019.

[141] X. Ge, J. Wang, J. Ding, X. Cao, Z. Zhang, J. Liu, and X. Li, "Combining UAV-based hyperspectral imagery and machine learning algorithms for soil moisture content monitoring," *PeerJ*, vol. 7, May 2019, Art. no. e6926.

[142] I. Hajdu, I. Yule, and M. H. Dehghan-Shear, "Modelling of near-surface soil moisture using machine learning and multi-temporal Sentinel 1 images in New Zealand," in *Proc. IEEE Int. Geosci. Remote Sens. Symp.*, Jul. 2018, pp. 1422–1425.

[143] J. Im, S. Park, J. Rhee, J. Baik, and M. Choi, "Downscaling of AMSR-E soil moisture with MODIS products using machine learning approaches," *Environ. Earth Sci.*, vol. 75, no. 15, pp. 1–19, Aug. 2016.

[144] I. Guyon and A. Elisseeff, "An introduction to variable and feature selection," *J. Mach. Learn. Res.*, vol. 3, pp. 1157–1182, May 2003.

[145] A. Singh, J. Amutha, J. Nagar, S. Sharma, and C.-C. Lee, "AutoML-ID: Automated machine learning model for intrusion detection using wireless sensor network," *Sci. Rep.*, vol. 12, no. 1, pp. 1–14, May 2022.

[146] W. Skierucha, A. Wilczek, A. Szypłowska, C. Sławiński, and K. Lamorski, "A TDR-based soil moisture monitoring system with simultaneous measurement of soil temperature and electrical conductivity," *Sensors*, vol. 12, no. 10, pp. 13545–13566, Oct. 2012.

[147] H. Mittelbach, I. Lehner, and S. I. Seneviratne, "Comparison of four soil moisture sensor types under field conditions in Switzerland," *J. Hydrol.*, vols. 430–431, pp. 39–49, Apr. 2012.

[148] J. C. Ryan, A. Hubbard, T. D. Irvine-Fynn, S. H. Doyle, J. M. Cook, M. Stibal, and J. E. Box, "How robust are in situ observations for validating satellite-derived albedo over the dark zone of the Greenland ice sheet?" *Geophys. Res. Lett.*, vol. 44, no. 12, pp. 6218–6225, Jun. 2017.

[149] K. K. Thakur, R. Vanderstichel, J. Barrell, H. Stryhn, T. Patanasatienkul, and C. W. Revie, "Comparison of remotely-sensed sea surface temperature and salinity products with in situ measurements from British Columbia, Canada," *Frontiers Mar. Sci.*, vol. 5, p. 121, Apr. 2018.

[150] W. Wagner, "Operational readiness of microwave remote sensing of soil moisture for hydrologic applications," *Hydrol. Res.*, vol. 38, no. 1, pp. 1–20, 2007.

[151] K. Das and P. K. Paul, "Present status of soil moisture estimation by microwave remote sensing," *Cogent Geosci.*, vol. 1, no. 1, Dec. 2015, Art. no. 1084669.

[152] L. Moser, A. Schmitt, A. Wendleder, and A. Roth, "Monitoring of the Lac Bam wetland extent using dual-polarized X-band SAR data," *Remote Sens.*, vol. 8, no. 4, p. 302, Apr. 2016.

[153] A. Schmitt, T. Leichtle, M. Huber, and A. Roth, "On the use of dual-co-polarized Terrasar-X data for wetland monitoring," *Int. Arch. Photogramm., Remote Sens. Spatial Inf. Sci.*, vol. XXXIX-B7, pp. 341–344, Aug. 2012.

[154] A. Singh, J. Nagar, S. Sharma, and V. Kotiyal, "A Gaussian process regression approach to predict the k-barrier coverage probability for intrusion detection in wireless sensor networks," *Expert Syst. Appl.*, vol. 172, Jun. 2021, Art. no. 114603.

[155] A. Singh, J. Amutha, J. Nagar, S. Sharma, and C.-C. Lee, "LT-FS-ID: Log-transformed feature learning and feature-scaling-based machine learning algorithms to predict the k-barriers for intrusion detection using wireless sensor network," *Sensors*, vol. 22, no. 3, p. 1070, Jan. 2022.

[156] A. Rácz, D. Bajusz, and K. Héberger, "Effect of dataset size and train/test split ratios in QSAR/QSPR multiclass classification," *Molecules*, vol. 26, no. 4, p. 1111, Feb. 2021.

[157] D. S. Prashanth, R. V. K. Mehta, and N. Sharma, "Classification of handwritten devanagari number—An analysis of pattern recognition tool using neural network and CNN," *Proc. Comput. Sci.*, vol. 167, pp. 2445–2457, Jan. 2020.

[158] X. He, K. Zhao, and X. Chu, "AutoML: A survey of the state-of-the-art," *Knowl.-Based Syst.*, vol. 212, Jan. 2021, Art. no. 106622.

[159] G. E. Karniadakis, "Physics-informed machine learning," *Nature Rev. Phys.*, vol. 3, no. 6, pp. 422–440, 2021.

[160] G. C. Topp, G. W. Parkin, T. P. Ferré, M. R. Carter, and E. G. Gregorich, "Soil water content," in *Soil and Environmental Analysis: Physical Methods*, K. A. Smith and C. E. Mullins, Eds. New York, NY, USA: Marcel Dekker, 2001, pp. 1–64.

[161] V. V. Kramarenko, A. N. Nikitenkov, V. Yu Molokov, A. V. Shramok, and G. P. Pozdeeva, "Application of microwave method for moisture determination of organic and organic-mineral soils," *IOP Conf. Ser., Earth Environ. Sci.*, vol. 33, Mar. 2016, Art. no. 012040.

[162] D. J. Belcher, "The measurements of soil moisture and density by neutron and gamma-ray scattering," U.S. Civil Aeronaut. Admin. Tech. Devel., New Delhi, India, Tech. Rep. 127, 1950.

[163] A. Klute and R. C. Dinauer, "Physical and mineralogical methods," *Planning*, vol. 8, p. 79, Jan. 1986.

[164] J. R. Mchenry, "Theory and application of neutron scattering in the measurement of soil moisture," *Soil Sci.*, vol. 95, no. 5, pp. 294–307, May 1963.

[165] T. J. Schmugge, T. J. Jackson, and H. L. McKim, "Survey of methods for soil moisture determination," *Water Resour. Res.*, vol. 16, no. 6, pp. 961–979, 1980.

[166] E. L. Greacen, "Soil water assessment by the neutron method," Division Soil, CSIRO, Adelaide, SA, Australia, Tech. Rep., 1981.

[167] D. S. Chanasyk and M. A. Naeth, "Field measurement of soil moisture using neutron probes," *Can. J. Soil Sci.*, vol. 76, no. 3, pp. 317–323, Aug. 1996.

[168] D. Cassel and T. Krueger, "Gamma rays determine soil water content of soil-plant systems," *Farm Res.*, vol. 29, no. 4, pp. 1–5, Mar/Apr. 1972.

[169] J. M. Baker and R. R. Allmaras, "System for automating and multiplexing soil moisture measurement by time-domain reflectometry," *Soil Sci. Soc. Amer. J.*, vol. 54, no. 1, pp. 1–6, Jan. 1990.

[170] S. B. Jones, J. M. Wraith, and D. Or, "Time domain reflectometry measurement principles and applications," *Hydrol. Process.*, vol. 16, no. 1, pp. 141–153, 2002.

[171] G. C. Topp, J. L. Davis, and A. P. Annan, "Electromagnetic determination of soil water content: Measurements in coaxial transmission lines," *Water Resour. Res.*, vol. 16, no. 3, pp. 574–582, Jun. 1980.

[172] M. Dobson, F. Ulaby, M. Hallikainen, and M. El-rayes, "Microwave dielectric behavior of wet soil—Part II: Dielectric mixing models," *IEEE Trans. Geosci. Remote Sens.*, vols. GE–23, no. 1, pp. 35–46, Jan. 1985.

[173] R. Chen, V. P. Drnevich, X. Yu, R. L. Nowack, and Y. Chen, "Time domain reflectometry surface reflections for dielectric constant in highly conductive soils," *J. Geotechnical Geoenvironmental Eng.*, vol. 133, no. 12, pp. 1597–1608, Dec. 2007.

[174] S. Jonnalagadda, "Resistivity and time domain reflectometry sensors for assessing in situ moisture content in a bioreactor landfill," Ph.D. dissertation, Univ. Florida, Gainesville, FL, USA, 2004.

[175] Z. Gao, Y. Zhu, C. Liu, H. Qian, W. Cao, and J. Ni, "Design and test of a soil profile moisture sensor based on sensitive soil layers," *Sensors*, vol. 18, no. 5, p. 1648, May 2018.

[176] Y. Chen and D. Or, "Effects of Maxwell–Wagner polarization on soil complex dielectric permittivity under variable temperature and electrical conductivity," *Water Resour. Res.*, vol. 42, no. 6, Jun. 2006, Art. no. W06424.

[177] R. Muñoz-Carpena, S. Shukla, and K. Morgan, *Field Devices for Monitoring Soil Water Content*, vol. 343. Gainesville, FL, USA: Univ. Florida Cooperative Extension Service, Institute of Food, 2004.

[178] S. Matula, K. Bát'ková, and W. Legese, "Laboratory performance of five selected soil moisture sensors applying factory and own calibration equations for two soil media of different bulk density and salinity levels," *Sensors*, vol. 16, no. 11, p. 1912, Nov. 2016.

[179] L. McCarty, *Golf Turf Management*. Boca Raton, FL, USA: CRC Press, 2018.

[180] L. A. Richards, "Soil moisture tensiometer materials and construction," *Soil Sci.*, vol. 53, no. 4, pp. 241–248, Apr. 1942.

[181] M. Thalheimer, "A low-cost electronic tensiometer system for continuous monitoring of soil water potential," *J. Agricult. Eng.*, vol. 44, no. 3, p. 16, Dec. 2013.

[182] G. J. Bouyoucos, *An Electrical Resistance Method for the Continuous Measurement of Soil Moisture Under Field Conditions*, vol. 172. East Lansing, MI, USA: Technical Bulletin. Michigan Agricultural Experiment Station, 1940.

[183] B. Richards, "Measurement of free energy of soil moisture by the psychrometric technique, using thermistors," Butterworth Company Ltd, London, U.K., Tech. Rep. 00237324, 1965.

[184] I. Rocchi, C. G. Gragnano, L. Govoni, A. Mentani, M. Bittelli, P. Castiglione, O. Buzzi, and G. Gottardi, "A new technique for deep in situ measurements of soil water retention behaviour," *Geotechnical Res.*, vol. 5, no. 1, pp. 3–12, Mar. 2018.
[185] Y. Oh, K. Sarabandi, and F. T. Ulaby, "An inversion algorithm for retrieving soil moisture and surface roughness from polarimetric radar observation," in *Proc. IEEE Int. Geosci. Remote Sens. Symp.*, vol. 3,Aug. 1994, pp. 1582–1584.
[186] Y. Oh and Y. C. Kay, "Condition for precise measurement of soil surface roughness," *IEEE Trans. Geosci. Remote Sens.*, vol. 36, no. 2, pp. 691–695, Mar. 1998.
[187] N. Baghdadi, P. Paillou, G. Grandjean, P. Dubois, and M. Davidson, "Relationship between profile length and roughness variables for natural surfaces," *Int. J. Remote Sens.*, vol. 21, no. 17, pp. 3375–3381, Jan. 2000.

ABHILASH SINGH (Member, IEEE) is currently pursuing the Ph.D. degree in remote sensing from the Indian Institute of Science Education and Research Bhopal, Bhopal, India. His current research interest includes coupling machine learning algorithms with satellite imagery to exploit satellite observations (soil moisture, surface roughness, river discharge, and disease prediction). He is a member of EGU, AGU, ISPRS, and the Indian Radio Science Society (InRaSS). He was a recipient of gold medal awards from the University for being a first-rank holder in his bachelor's and master's. He received the prestigious "DST-INSPIRE" Fellowship to carry out his doctoral degree from the Department of Science and Technology (DST), India's Ministry of Science and Technology. He also received the DAAD Fellowship, a travel grant from American Geophysical Union (AGU), Early Career Scientists Travel Support from European Geophysical Union (EGU), and AGU Ecohydrology Early Career Tiny Grant.

KUMAR GAURAV received the M.Sc. degree in geoinformatics from the Indian Institute of Remote Sensing (IIRS) and the University of Twente (ITC), The Netherlands, in 2009, and the Ph.D. degree from the Geological Fluid Dynamics Laboratory, Institut de Physique du Globe de Paris (IPGP), in 2016. He is currently working as an Assistant Professor with the Department of Earth and Environmental Sciences, Indian Institute of Science Education and Research Bhopal, India. He is a geomorphologist working on fluvial problematic. He is interested in learning rivers' dynamics and morphology, drainage congestion's effect on flood inundation, and the application of remote sensing to monitor soil moisture and stream flow. He combines mathematical theory, physical reasoning, field observations, machine learning, and digital image analysis to recognize the necessary ingredients to model them.

GAURAV KAILASH SONKAR received the master's degree in environmental science from the Fergusson College (Savitribai Phule Pune University), Pune, India, in 2015. He is currently pursuing the Ph.D. degree in river eco-geomorphology from the Indian Institute of Science Education and Research Bhopal, India. He is working on the impact assessment of human intervention on river landscape habitat. He has been publishing research papers in international conferences and reputed journals. His recent research interest includes integrating multiple disciplines at relevant scales to assess and understand the cause-and-effect dynamics in the riverine habitats of recent times. He received the UGC–Junior Research Fellowship to pursue his Ph.D. degree from the UGC, Government of India. He is a member of the EGU and ISPRS.

CHENG-CHI LEE (Member, IEEE) received the Ph.D. degree in computer science from the National Chung Hsing University (NCHU), Taiwan, in 2007. He is currently a Distinguished Professor with the Department of Library and Information Science, Fu Jen Catholic University. His current research interests include data security, cryptography, network security, mobile communications and computing, and wireless communications. He has published over 200 articles on the above research fields in international journals. He is a member of the Chinese Cryptology and Information Security Association (CCISA), the Library Association of The Republic of China; and the ROC Phi Tau Phi Scholastic Honor Society. He is also an editorial board member of some journals. He also served as a reviewer in many SCI-Index journals, other journals, and other conferences.